Taxonomic re-examination of the toxic armored dinoflagellate Pyrodinium bahamense Plate 1906: Can morphology or LSU sequencing separate P. bahamense var. compressum from var. bahamense?

Citation	Mertens, K. N., Wolny, J., Carbonell-Moore, C., Bogus, K., Ellegaard, M., Limoges, A., ... & Matsuoka, K. (2015). Taxonomic re-examination of the toxic armored dinoflagellate Pyrodinium bahamense Plate 1906: Can morphology or LSU sequencing separate P. bahamense var. compressum from var. bahamense?. Harmful Algae, 41, 1-24. doi:10.1016/j.hal.2014.09.010
DOI	10.1016/j.hal.2014.09.010
Publisher	Elsevier
Version	Accepted Manuscript
Terms of Use	http://cdss.library.oregonstate.edu/sa-termsofuse

Taxonomic re-examination of the toxic armoured dinoflagellate *Pyrodinium bahamense* Plate 1906: can morphology or LSU sequencing separate *P. bahamense* var. *compressum* from var. *bahamense*?

Kenneth Neil Mertens (kenneth.mertens@ugent.be) [corresponding author]
Research Unit for Palaeontology, Gent University, Krijgslaan 281 s8, 9000 Gent, Belgium

Jennifer Wolny (Jennifer.Wolny@maryland.gov)
University of South Florida, Fish and Wildlife Research Institute, 100 Eighth Avenue SE, St. Petersburg, Florida 33701, USA*
*present address: Maryland Department of Natural Resources, 1919 Lincoln Drive, Annapolis, MD 21401, USA

Consuelo Carbonell-Moore (carbonem@onid.orst.edu)
Department of Botany and Plant Pathology, College of Agricultural Sciences, Oregon State University, Corvallis, OR 97331-2902, U.S.A.

Kara Bogus (bogus@iodp.tamu.edu)
International Ocean Discovery Program and Department of Geology and Geophysics, Texas A&M University, 1000 Discovery Drive, College Station, TX 77845, USA

Marianne Ellegaard (me@plen.ku.dk)
Department of Plant and Environmental Sciences, Faculty of Science, University of Copenhagen, Thorvaldsensvej 40 1st floor DK-1871 Frederiksberg C Denmark

Audrey Limoges (limoges.audrey@gmail.com)
GEOTOP, Université du Québec à Montréal, P.O. Box 8888, Montréal, Québec, H3C 3P8, Canada

Anne de Vernal (devernal.anne@uqam.ca)
GEOTOP, Université du Québec à Montréal, P.O. Box 8888, Montréal, Québec, H3C 3P8, Canada

Pieter Gurdebeke (pieter.gurdebeke@ugent.be)
Research Unit for Palaeontology, Gent University, Krijgslaan 281 s8, 9000 Gent, Belgium

Takuo Omura (omura@lasc.co.jp)
Laboratory of Aquatic Science Consultant Co., LTD. (LASC), 1-14-1, Kami-ikedai, Ota-ku, 145-0064, Tokyo, Japan

Abdulrahman Al-Muftah (aralmuftah@qu.edu.qa)
Qatar University, Department of Biological and Environmental Sciences, Doah,Qatar

Kazumi Matsuoka (kazu-mtk@nagasaki-u.ac.jp)
Institute for East China Sea Research (ECSER), 1551-7 Taira-machi, Nagasaki, 852-8521, Japan

Abstract

Pyrodinium bahamense Plate 1906 is a tropical to subtropical dinoflagellate that can cause paralytic shellfish poisoning (PSP). Based on differences in the morphology of the motile stage, as well as geographic distribution, this species was separated into two varieties, the toxic var. *compressum* and the non-toxic var. *bahamense* by Steidinger et al. (1980). Thereafter, Balech (1985) carefully reinvestigated the two varieties and concluded there were no significant morphological differences between them. We re-examined the motile cell and cyst morphology of these two varieties, concurring with the arrangement of the sulcal plates, but demonstrating the plate overlap for the first time. The observed size-frequency spectra of cell body diameter, cyst body diameter and cyst process length were unimodal. Overall, we agree with Balech (1985) that there is no consistent criterion to unequivocally separate both varieties based on morphology. We therefore recommend ceasing the use of these varieties (and forma). In addition, we suggest that observations of both varieties in a single plankton sample should be interpreted as the occurrence of different life stages at the sampling time. However, the phylogenetic analysis using

partial LSU rDNA sequence data revealed two clearly separated ribotypes within the *Pyrodinium* clade, an Indo-Pacific and Atlantic-Caribbean ribotype, suggesting that *Pyrodinium bahamense* is a species complex. The genetic distance between these ribotypes is short, which suggests a late Quaternary separation. Geochemical analyses of the cyst walls also show differences between specimens from both geographical regions.

Keywords

Biometry, cyst, theca, thermophile, LSU, saxitoxins

1. Introduction

The armoured dinoflagellate, *Pyrodinium bahamense* Plate 1906 is one of the most important harmful algal bloom (HAB) organisms in South Asian coastal waters (e.g., Usup et al., 2012). In 1972, paralytic shellfish poisoning (PSP) occurred near Port Moresby (Papua New Guinea) where *P. bahamense* was considered to be the causative organism for that event (Maclean, 1973; Worth et al., 1975). This was the first recognition of a PSP incident caused by *P. bahamense* in Southeast Asia. Since then, toxic blooms associated with PSP have been reported throughout Southeast Asia, in particular Malaysia (e.g., Roy, 1977), Papua New Guinea (e.g., Maclean, 1989), the Philippines (e.g., Gonzales, 1989), Brunei (e.g., Jaafar et al., 1989) and Indonesia (e.g., Wiadnyana et al., 1996) as well as the Pacific coast of Central America (e.g., Guatemala, Rosales-Loessener, 1989).

Pyrodinium bahamense was originally described from the Atlantic, specifically New Providence Island (Bahamas) by Plate (1906). Later, Böhm (1931) described from one *P. bahamense* cell from the Red Sea as forma *compressa*, based upon the fact that its body was wider than longer, and that it had only a long “antapical spine.” Since then, it has been widely accepted that the Indo-Pacific populations would fall into forma *compressa*, while the Atlantic populations would correspond to the forma *bahamense*, or the “form” originally described by Plate. It was not until the first PSP outbreak in Papua New Guinea in the early 1970s caused by *Pyrodinium bahamense* (Maclean, 1973) that toxicity was added to the “apparent” differences between the two

P. bahamense forms. Steidinger et al. (1980) elevated the form status to variety on the basis of morphological criteria for the motile stage and the capability of PSP toxin production. This separation was supported at the time by the biogeographic distribution of both varieties: var. *compressum* was apparently endemic to the Pacific and Indian oceans, while var. *bahamense* occurred in the Caribbean Sea and the Atlantic Ocean. Both var. *bahamense* (Wall and Dale, 1969) and var. *compressum* (Matsuoka, 1989) produce resting cysts that preserve in the sediment, and Matsuoka (1989) reported that process length and body diameter showed significant differences between both varieties.

However, differentiation between the two varieties based on morphological criteria is not unequivocal as shown by Balech (1985) in a detailed morphological analysis of thecae comprising populations from Papua New Guinea, the Philippines, Jamaica and Puerto Rico. Moreover, the physiological criterion of toxin production *versus* non-production is no longer applicable because cultures isolated from Florida by Landsberg et al. (2006) showed that PSP causing toxins, *in casu* saxitoxins, can be produced by var. *bahamense*. Finally, the segregated biogeography is no longer supported as both varieties have been reported to co-occur in several locations such as Costa Rica (Vargas-Montero and Freer, 2003), the Pacific coast of Mexico (Gárate-Lizárraga and González-Armas, 2011) and the Arabian Gulf (Glibert et al., 2002).

In this study, we provide a multi-approach investigation into whether *Pyrodinium bahamense* can be unambiguously separated through: (1) measurements of morphological variation for both individual motile cells and cysts, (2) geochemical analyses of the resting cyst walls, and (3) phylogenetic analysis based on partial large subunit (LSU) ribosomal DNA sequences. Based on our results, we discuss the taxonomic position of *P. bahamense* var. *bahamense* and var. *compressum,* in the context of toxicity and biogeography, and recommend that the use of varieties be discontinued. In addition, the underlying factors producing morphological variability and phylogenetic separation are discussed.

2. Material and methods

2.1. Plankton sample localities and motile stage study and measurements

Thecate motile stages of *Pyrodinium* examined in this study were collected using a 20 µm plankton-net from 13 coastal areas of various tropical and subtropical waters in Southeast Asia, Qatar, the Atlantic coast of Guatemala, the Floridian Atlantic, the Gulf of Mexico, and the Caribbean (Fig. 1A, Table 1). The vegetative cells were examined by K.N.M., K.M. and J.W. under normal light and/or interference microscope(s) (Zeiss Axiophoto and Olympus IX71 equipped with an Olympus DP71 digital camera). Plate terminology in general followed Fensome et al. (1993); we indicate in the results when it did not. Each specimen was oriented in ventral or dorsal view, focused on the cross-section, and the body length (measured along the apical-antapical axis, excluding the apical horn) and width (measured along the cingulum, excluding the cingular lists) were measured (Fig. 2A). Between nine and 116 cells were measured in each sample (Table 2). The W/L ratio was calculated by dividing the body width by length.

For scanning electron microscopy (SEM) by C.C.M., samples were prepared either by filtering a sample, or isolating a single cell under the light microscope. When the sample was filtered, an aliquot of ~300 µL was placed on a Millipore ™ 0.25 mm diameter-5 µm pore polycarbonate filter at the bottom of a Millipore™ column. Approximately 7 ml of distilled water were added to remove fixative (lugol or formaldehyde) and seawater. Gentle manual vacuum with a 60 cc syringe was used to speed filtration. Individually isolated cells were removed using a glass micropipette under a Leica Inverted Light Microscope (Germany) with magnification 10x5x. Individual cells were washed six times with distilled water in double depression microscope slides). After the cells were clean, they were placed on the same kind of filter as for the filtered samples. All filters were air-dried, then adhered to 25 mm diameter aluminum stubs with adhesive tabs (7/16" diameter). The mounted filters were then coated with a mixture of gold-palladium in a Cressington Sputter Coater (U.S.A.) for 60 s. Observations were performed with a FEI Quanta 3D Dual Beam SEM (Clackamas, Oregon, U.S.A.), at 5 kV. Tilts up to 52° were applied. Digital images were saved in Tiff format (2048 x 1768 pixels). K.N.M. used a different protocol: plankton samples were rinsed with distilled water to remove the salts and fixative. Strew slides were made from the residue and were air-dried, sputter-coated with palladium, and observed using a Hitachi S-3400N SEM. In both cases, Adobe-Photoshop™ software was used to remove the background while maintaining the integrity of the original image.

2.2. Establishment of cultures

The *Pyrodinium* cultures intended for reproductive physiology were established from plankton samples collected with a 20 µm plankton net from the Pacific (Masinloc, Palawan and Sorsogon (Philippines)) and the Atlantic (Vieques Island (Puerto Rico), Terra Ceia, Tampa Bay and Indian River Lagoon (Florida)) by T.O. and J.W. (Fig. 1A, Table 1). Isolates, except those from Florida, were grown in modified T1 medium (Ogata et al., 1987) at 26°C, irradiance of 100-125 µmol photons m^{-2} s^{-1}, and a light:dark cycle of 12:12 h. Similar measurements were made as for the plankton samples. Florida isolates were grown at 35 µEinstein/m^2/sec, 25°C and at salinities of 20–36 psu (depending on the strain), in ES-DK medium (Kokinos and Anderson, 1995) with the addition of 10^{-7} M selenium (as sodium selenite).

2.3. Cysts extracted from surface sediment: sample preparation, light microscopy, scanning electron microscopy and micro-Fourier transform spectroscopy

Cyst measurements were carried out on specimens recovered from 43 globally distributed surface sediments (Fig. 1B; Table 2). Most samples were core top samples obtained from areas with relatively high sedimentation rates (see references in Table 2). They represent tens of years to a few centuries. All of the cysts were extracted by K.N.M., K.M. and P.G. from the sediments using standard palynological methods involving hydrochloric acid and hydrofluoric acid, sieving and/or sonication (Table 2). Residue aliquots were mounted in glycerine gelatin.

All measurements and light photomicrographs were made by K.N.M. and K.M. using an Olympus BX51 with a Nikon digital sight DS-1L 1 module, a Nikon Eclipse 80i microscope and coupled Nikon DS Camera Head (DS-Fi1) /DS Camera Control Unit DS-L2, all with 100x oil immersion objectives. For each sample, between 13 and 50 cysts were measured for body diameter and the length of the three longest visible processes on each cyst (Fig. 2B). Measuring 50 cysts yields reproducible results (Mertens et al., 2011) with average process length per sample being reliably reproduced (±0.5 µm) among observers. Process length was measured from the middle of the process base to the tip. To reduce the possibility of observer-dependent bias, only specimens carrying processes with characteristic aculeate distal ends were measured for the morphological analysis. For each cyst, three processes were always found within the focal plane of the light microscope at the optical section of the central cyst body, and thus this number seemed a reasonable option. The reasons for choosing to measure the longest processes were (1) the longest processes reflect unobstructed cyst growth, (2) measuring the longest processes increases the accuracy of the proxy as it documents the largest variation, (3) since only a few processes were parallel to the focal plane of the microscope, it was imperative to make a consistent choice. Fragments representing less than half of a cyst were not measured, nor were cysts with mostly broken processes.

For scanning electron microscopy (SEM) by K.M. and M.E., palynological residues were filtered and washed with distilled water and dehydrated in a graded ethanol series (30 to 100% in six steps). The filters were encased in metallic baskets, critical-point-dried with CO_2 (CPD Bal-Tec 030), glued onto stubs, sputter coated with platinum/palladium for 90 s (JEOL JFC-2300 HR) and examined in a JEOL 6330F scanning electron microscope (JEOL, Tokyo, Japan).

Geochemical measurements of resting cyst walls were performed by K.B. with micro-Fourier transform infrared (FTIR) spectroscopy using three cyst residues from two regions, Indonesia (Ambon (St. 10) and Kao Bay (KAB 14A)) and Florida (West Lake 25) (Fig. 1B; Table 2). Residues were briefly ultrasonicated (60 s), sieved over 10 µm mesh, and then soaked (30 min) in a dichloromethane (DCM) and methanol (MeOH) solution (1:1 *v:v*). This step was to remove any extraneous lipid compounds on the cyst walls. The residues were then ultrasonicated (60 s) and rinsed three times with Milli-Q water. Individual specimens were isolated and dried overnight. Four to six specimens from each sample were analyzed; specimens from Indonesia (Ambon and Kao Bay) represent var. *compressum* and specimens from Florida (West Lake), var. *bahamense*. Analyses were performed on a Nicolet FT-IR spectrometer coupled to a Nicplan microscope with 256 scans obtained in transmission mode at 4 cm^{-1} resolution over a spectral range of 4000-650 cm^{-1}. All reported spectra depict the sample beam following subtraction of the background (NaCl plate + air). Assignments of the characteristic IR group frequencies were made using Colthup et al. (1990) and published literature (e.g., Versteegh et al., 2012; Bogus et al., 2014).

2.4. Environmental data

Seasonal and annual sea surface temperature (SST), sea surface salinity (SSS), and sea surface density (σ_t) were interpolated using the gridded 1/4 degree World Ocean Atlas (WOA) 2001 (Conkright et al., 2002) and the Ocean Data View software (Schlitzer, 2012). The WOA 2001 is generated from the World Ocean Database 2001, which covers 7.9 million data points of historical and modern oceanographic data. We used the WOA 2001 since it has a 1/4 degree resolution. For the Florida sites (Tampa Bay, West Lake and Safety Harbor), we used *in situ* measurements. Biometric measurements of cysts from the various study areas were compared to SST, SSS, and σ_t by calculating the coefficient of determination R^2. The significance of R^2 was calculated using a t-test. We did not compare the body lengths of the motile stages to the environmental parameters because only 12 samples were measured.

2.5. Single-cell PCR amplification and sequencing

Single-cell PCR amplification was conducted by T.O. on motile cells of *Pyrodinium bahamense* collected from Vieques Island (Puerto Rico) and Manila Bay and Masinloc Bay (the Philippines). Partial LSU (D1-D2) rDNA sequences were amplified from a single cell according to the procedure of Iwataki et al. (2007). After microscopic observations, motile cells were broken with a sharp glass rod and their contents transferred to a 200 µL tube containing 10 µL distilled water. 20 µL was used for PCR amplification according to the manufacturer's recommendation of KOD-Plus-DNA Polymerase (Toyobo, Osaka, Japan) on a GeneAmp 9600 PCR System (Perkin-Elmer, Foster City, USA). Terminal primers for amplification of LSU rDNA were D1R and D2C (Scholin et al., 1994). The PCR reactions were performed in two steps. The first round of PCR consisted of an initial denaturation at 95°C for 10 min, followed by 35 cycles of 95°C for 1 min, 55°C for 1 min, and 72°C for 3 min. The reaction was completed with a final elongation at 72°C for 10 min. The second round of PCR using the first PCR product consisted of an initial denaturation at 95°C for 10 min, followed by 40 cycles of 94°C for 30 s, 55°C for 30 s, and 72°C for 30 s. The reaction was completed with a final extension at 72°C for 10 min. The PCR product was purified using a Microcon YM-100 Centrifugal Filter Device (Millipore, Billerica, MA, USA), and the cycle-sequencing reaction was performed using an ABI PRISM BigDye™

Terminator v3.1 Cycle Sequencing Kit (Perkin-Elmer) following the manufacturer's protocol. Sequencing was run on an ABI PRISM 377 Sequencer (Perkin-Elmer) with the PCR primer set and internal primers.

For cultures established from Oyster Bay (Jamaica) and Tampa Bay and Indian River Lagoon (Florida, U.S.A.), 5 ml of culture was centrifuged at 13,000 rpm for 2 min and DNA was isolated with the Puragene extraction kit (Qiagen). The primers used were D1R and D2C (Scholin et al., 1994). PCR conditions consisted of an initial denaturation at 94°C for 2 min, followed by 35 cycles of 94°C for 30 s, 55°C for 30 s, 72°C for 3 s, and a final extension of 72°C for 7 min. The PCR product was purified with the PCR Purification kit (Qiagen). Cycle sequencing reactions were performed with a Big Dye Terminator v3.1 cycle sequencing kit (Applied Biosystems) and run on an ABI 3130XL genetic analyzer (Applied Biosystems).

The sequences can be obtained from GenBank under accession numbers of AB936754-AB936755 and AB970714-AB970721.

2.6. Sequence alignments and phylogenetic analyses

The sequences determined in this study and selected from DDBJ/EMBL/GenBank were automatically aligned with the Clustal W 2.1 computer algorithm. Phylogenetic trees for maximum-parsimony (MP), neighbor-joining (NJ) and maximum-likelihood (ML) methods were constructed using using MEGA version 5 (Tamura et al., 2011). For LSU rDNA sequences, TrN+G (α=0.5012) with base frequencies A=0.2258, C=0.2047, G=0.3043, T=0.2652, and substitution rate matrix with A–G=1.5785, C–T=4.9203, were selected. Bootstrap support values (Felsenstein, 1985) were estimated for NJ (1000 replicates), MP (1000 replicates) and ML trees (1000 replicates). We calculated genetic distance using the Maximum Composite Likelihood model (Tamura et al., 2004) using the software package MEGA5 (Tamura et al., 2011).

3. Results

3.1. Morphological observations of the motile stages of *Pyrodinium bahamense*

The observed plate formula (PO, PI, 4′, 0a, 6″, 6c, 9s, 5‴, 1p, 1⁗) is in close agreement with previous studies documenting the morphology of *Pyrodinium bahamense*, except for the number of sulcal plates (e.g., Steidinger et al., 1980; Badylak et al., 2004; Morquecho, 2008), and is in complete agreement with Balech (1985). We did not observe any variation in the tabulation. Rarely, five apical plates have been observed in other studies (see below). We also successfully documented the plate overlap of this species (Fig. 3). However, our SEM examination of numerous *Pyrodinium bahamense* cells from different localities (see Table 1, Suppl. Plates 2-6) found several discrepancies with previous observations, which are discussed below.

3.1.1. Apical pore complex

We confirmed that the apical pore complex is correctly described by Balech (1985) as formed by two separate plates: the pore plate (PO) and the closing or cover plate (PI) (Plates 1-2). This contradicts Taylor and Fukuyo (1989, p. 215), who stated that the plates could not be separated. The PO showed significant variation in the size and number of pores. In some cells, one of these pores became much larger, and functioned most likely as an attachment pore (Plate 1A, B, 2A). The size of PI also varied according to the presence of this attachment pore. When this pore was absent, the PO was large (Plate 1C, E), while the PO was much narrower than when an attachment pore was present (Plate 1A,B). Examples of large POs can be observed in large cells, with wide growth bands (see 3.1.2) (Plate 3A-B, 4B, C, E,F, H, I). The multiple drawings given by Balech (1985, his Plate I, Figs. 21, 22, his Plate III, Fig. 33, his Plate IV, Figs. 60-62) depict an attachment pore separated from the inner side the PO (Plate 2B). However, our observations showed that this pore abuts the PO, with no physical separation between them (Plate 1A-E, 2A). Balech's drawings suggest that he had viewed the inside of the plate and not the outside (cf. Plate 2C, D), which is common in observations made under the light microscope. A comparison of his drawings (Balech 1985, his Plate IV, Fig. 61; redrawn here in Plate 2B), with our SEM images of the inside of the epitheca (Plate 2C, D) demonstrates why Balech drew a gap between the PI and the attachment pore (Plate 2B).

Additionally, the representation of the apical pore given by Plate (1906) in his Figure 11 of the original description of *Pyrodinium bahamense* is not only seen through the cell and is inverted (apex down), but also depicts the apical pore of a species of *Goniodoma* Stein, another common dinoflagellate found around the Bahamas. Plate (1906, p. 421) highlighted this finding as an unusual apical pore in one cell, which was perpendicular to the dorsoventral axis, while this pore was diagonal in all other cells. In *Goniodoma*, the apical pore complex is situated as described by Plate (1906). This is supported by the findings of Fukuyo and Taylor (1980), which highlighted the similarity between both dinoflagellates (*Goniodoma polyedricum* and *Pyrodinium bahamense*) and described how they can be misidentified by the untrained eye using light microscopy.

3.1.2. Lists, spines and growth bands

Pyrodinium bahamense may develop quite elaborate lists along the sutures of the apical, sulcal and cingular plates (Plates 3-7). These lists are extensions of the thecal plates and in a similar fashion to the plates, they are covered by tiny spinulae (e.g., Plate 6D, E). A common mistake in the literature is to depict the apical list and spine, when present, on the dorsal part of the cell (e.g., Balech, 1985, his Plate I, Figs. 1, 2, 4, 8), Since they are located between plates 3′ and 4′, they are on the ventral part (e.g., Plate 6A-C) as correctly depicted by Plate (1906). Although Balech (1985, p. 29) did not find specimens with apical spines in the material that he examined from the Philippines, we did observe them (Plate 6B, C).

Furthermore, the left lateral list, as seen in Plate (1906, his Fig. 1), is most likely a growth band, which extend outwards, perpendicular to the surface of the plates (e.g., Plate 6B).

3.1.3. Sulcal plates

Sulcal plate nomenclature followed Balech (1985), where the left anterior sulcal plate (Ssa) corresponds to the first precingular plate of Kofoid (1909). The sulcal plates were thoroughly described by Balech (1985) who dissected multiple specimens of *Pyrodinium bahamense*. Our results confirm the presence of nine plates described by Balech (Fig. 4, Plates 8-9). In addition, this study presents a more comprehensive description of the sulcal plate arrangement than Balech (1985). The sulcal area is sunken, and half of the plates are hidden under the list of plates 1p and 5‴ (Plate 8). Balech's observations included plates that were dissected and not in their original position. Thanks to SEM observations of the inside of several hypothecae (Plate.10B-C), we were able to establish the arrangement of the posterior part of the sulcus, as well as detect the presence of a previously undescribed second flagellum pore located midway between plates Ssp and Sdp (Fig. 4). Plate 9 gives a perspective of the sulcal area in *Pyrodinium bahamense.* It is important to mention that the sulcal median plates do not fill most of the notch of the anterior sulcal plate as stated by Balech (1985, p.24), but rather fill the anterior gap between the left and right sulcal plates (Fig. 4, Plates 8-9). Also, as with the attachment pore on the apical pore plate, the posterior sulcal plate (Sp) may or may not bear an attachment pore, as previously illustrated by Balech (1985, his Plate IV, Figs. 69, 70) (Plate 5C, E). Likewise, large cells did not show a posterior attachment pore on the Sd plate (Plate 5C).

3.2. Are there differences in the morphology of the motile stage of *Pyrodinium bahamense*?

The two varieties of *P. bahamense*, var. *compressum* and var. *bahamense,* were distinguished by morphological criteria by Steidinger et al. (1980) using specific characteristics, which we evaluated. First, we present the results on the variability in body length (3.2.1), and then discuss if our observations support the proposed morphological characteristics of Steidinger et al. (1980) to differentiate var. *compressum* from var. *bahamense*: the ability to form chains (3.2.2), its anterior-posterior compression (3.2.3), the presence of a broad apical horn as well as the lack of an antapical spine and list system (3.2.4), the size of the trichocyst pores (3.2.5) and the presence of four to five apical plates (3.2.6). They were also originally considered biogeographically distinct. For this reason, we grouped the investigated samples into two major biogeographic regions based the varieties' original expected occurrence, the Atlantic-Caribbean and the Indo-Pacific. However, an unambiguous separation of both types was not always possible because the analysed specimen traits intergraded between the two end-members.

3.2.1. Size and shape differences

For the 12 globally distributed samples (Fig. 1A), the 760 length measurements averaged 46.01 µm (ranging between 27.30 and 81.78 µm) with a standard deviation of 9.35 µm. The 760 width measurements gave an average body diameter of 48.11 µm (ranging between 22.60 and 83.34 µm) with a standard deviation of 8.97 µm. In general, specimens from Florida and the Philippines were shorter, while specimens from Qatar and the Caribbean were longer (Fig. 5). The measurements indicated that in both regions there were specimens corresponding to the description of var. *bahamense* and var. *compressum.* They also showed intergradation of the two varieties in body length, shown by the unimodal distribution in the size-frequency spectra of the total dataset (Fig. 5). Therefore, body length is an unreliable criterion to unambiguously differentiate the two varieties. It is also important to note that within the samples a large variation in cell size is observed; these cells possibly correspond to different stages such as gametes, vegetative cells, planozygotes or even planomeiocytes (Suppl. Plates 1-6; see 4.3).

3.2.2. Chain formation ability

In Indo-Pacific plankton samples, *Pyrodinium bahamense* was usually observed as cell-chains consisting of more than four cells (Suppl. Plate 7D), but also as doublets (Suppl. Plate 7C) or solitary cells (Suppl. Plate 7A-B). Specimens observed in plankton samples from Kao Bay and Palau Island (Indo-Pacific) formed chains consisting of more than eight cells. In contrast, the cells from the Atlantic-Caribbean generally occurred as single cells in plankton samples (Suppl. Plate 8A, B, D; 9A-C), but were occasionally found as doublets (Suppl. Plate 8C, 9D). Specimens from Florida were also generally observed as single cells, occasionally as doublets; however, during blooms, chains of up to four cells were observed, as previously observed by Badylak et al. (2004).

Cultures from the Indo-Pacific generally grew as single cells (Suppl. Plate 10A-B) and cell-chains of two or four cells were rarely observed during the exponential growth phase (Suppl. Plate 10C-D). Under the same culture conditions, strains from the Atlantic-Caribbean generally grew as single cells (Suppl. Plate 10A-C) and rarely formed chains consisting of two cells (Suppl. Plate 10D), similar to the plankton samples. Comparable observations were made for cultures from Florida.

Therefore, this criterion clearly does not allow an unequivocal separation of two varieties.

3.2.3. Cell compression

When comparing the length and width of vegetative cells from plankton samples from the Atlantic-Caribbean and the Indo-Pacific regions, there was a strong overlap (Fig. 6). Therefore, compression cannot be used to unambiguously differentiate the two morphotypes. The cell compression was clearly related to cell-chain formation. Compressed forms, indicated by a high W/L ratio, were frequently observed in Pacific specimens that formed chains consisting of more than eight cells. Cell sizes from such samples were variable depending on the positions within the chain: intermediate cells were more compressed, while cells at the posterior and anterior ends were more spherical. Similar observations were made for chain forming cells from Florida, as well as for the established cultures.

3.2.4. Apical horn and antapical spines

The development of the apical horn and antapical spines was variable and, for chain-forming specimens, also largely dependent on the cell's position in a chain. The apical node is formed by the development of the perpendicular membranes surrounding the apical pore plate (Plate 3). In cells with an intermediate position in a chain, the apical horn was reduced (Suppl. Plate 8C, 7C-D, 10C-D) along with the antapical spines (Suppl. Plate 7C-D). However, the anterior cell in the chain had a more prominent apical horn, and the cell at the posterior end of the chain had typical antapical spines (Suppl. Plate 7A-B). Also, single cells from the Indo-Pacific were ellipsoidal and possessed a normal apical horn and antapical spines (Suppl. Plate 7A). Similarly, the ellipsoidal, often more elongated, single cells from the Atlantic-Caribbean usually possessed a well-developed apical horn originating from the membranous sutures (Suppl. Plate 8A-B). The variability of these characteristics shows that this is not conclusive in robustly differentiating both varieties.

3.2.5. Differences in trichocyst pore size

Steidinger et al. (1980) also considered the size of the trichocyst pores a possible characteristic to separate both varieties because var. *compressum* specimens have large pores (0.6-0.8 µm) and var. *bahamense* specimens have smaller pores (0.25-0.3 µm). However, Balech (1985) considered this variation to be mainly related to thickness of the thecal plates and did not notice consistent differences between both varieties. We made similar observations (Plate 7E,F) and therefore, chose not to investigate this further.

3.2.6. Presence of four or five apical plates

Several authors have observed rare specimens of *P. bahamense* with five apical plates in specimens identified as var. *compressum* (Matzenauer, 1933; Osorio Tafall, 1942; Taylor, 1976; Steidinger et al., 1980; Balech, 1985) and specimens identified as var. *bahamense* (Balech, 1985). In this study we did not observe any such specimens. In conclusion, this criterion is not useful to distinguish both varieties, and we have not investigated this further.

3.3. Morphological and geochemical differences in the cyst stage of *Pyrodinium bahamense* and the relationship to environmental parameters

First, we provide a general description of the cyst morphology (3.3.1) and describe the morphological measurements (3.3.2). Subsequently we present the cyst wall chemistry (3.3.3) and discuss how both morphology and geochemistry relate to the environmental parameters (3.3.4).

3.3.1. Morphological description of cysts of *Pyrodinium bahamense*

The analysed cysts were ellipsoidal in shape, and compressed along the anteroposterior axis (Plate 11B-C). The cyst walls were transparent and rather thick, varying between 1-3 µm. The inside of the inner cyst wall (pedium) was smooth, as seen under SEM (Plate 8A). The texture of the outer cyst wall was micrangranular to granular, with the luxuria forming inter-connecting fibrils and angular granules (Plate 11I, 12J). Processes were numerous (Plate 11B, 12B), intratabular (Plate 12C) and fibrous (Plate 11F, 12E-H). The processes were hollow (Plate 11F, 12I) with open and aculeate distal ends (Plate 11F, 12D, F, H). Rarely, processes were truncated, ending with blunt terminations (Plate 12D-E). Process bases were circular to oval (Plate 11I). Process length and width varied between two end-members, one bearing long, slender and tubiform processes (Plate 11A-B, 11F, 12A-B,D-E) and the other bearing short, broad and cylindrical processes (Plate 11C, 12C, G-H). Often, crests at the bases connected some processes. This most commonly occurred between two processes (Plate 11B, F, 12D), but, rarely, three processes were connected (Plate 11E, 12E). Connections also occurred along the length of the processes, which formed claustra at the base (Plate 11H, 12E). The archeopyle was saphopylic and epicystal, and consisted of four apical plates, the apical pore complex and six precingular plates (Plate 11G, 12A). A prominent sulcal notch was visible in the epicyst, formed by the anterior sulcal plate (Plate 11K). Paratabulation was usually visible on the epicyst (Plate 12C). Occasionally, cysts contained cell contents and had a bright, birefringent endospore below the cyst wall (Plate 11J). Occasionally, specimens were compressed or torn due to weathering.

3.3.2. Cyst biometrics

The observed cyst morphological traits also intergraded between two end-members. Similar to the motile stage measurements, we grouped them into the two major biogeographic regions, the Atlantic-Caribbean and the Indo-Pacific. For all 43 globally distributed samples (Fig. 1B), the 3,408 process length measurements averaged 9.42 μm (ranging from 2.51-21.75 μm) with a standard deviation of 2.27 μm. The 1,255 body diameter measurements resulted in an average body diameter of 53.50 μm (ranging from 31.12-84.80 μm) with a standard deviation of 6.26 μm. For the 19 samples from the Atlantic-Caribbean, the 1,170 process length measurements averaged 8.66 μm (ranging from 2.51-21.75 μm) with a standard deviation of 2.34 μm. The 506 body diameter measurements resulted in an average body diameter of 52.70 μm (ranging from 34.56-75.22 μm) with a standard deviation of 5.36 μm. For the 24 samples from the Indo-Pacific, the 2,238 process length measurements averaged 9.82 μm (ranging from 4.08-18.88 μm) with a standard deviation of 2.13 μm. The 749 body diameter measurements gave an average body diameter of 54.04 μm (ranging from 31.12-84.80 μm) with a standard deviation of 6.74 μm. All size-frequency curves of process length are unimodal, which is less pronounced for body diameter (Fig. 7). Atlantic-Caribbean specimens are on average, slightly smaller in body size and bear slightly shorter processes than their Indo-Pacific counterparts.

3.3.3. Correlation between environmental parameters, average process length and average cyst body diameter

All samples containing fewer than 10 measured cysts (9 of the 44 samples) were excluded from the analysis. The coefficient of determination R^2 was calculated between average process length and average body diameter and SSS, SST and σ_t of the surface water, both annually and seasonally for the Atlantic-Caribbean (16 samples), the Indo-Pacific (19 samples) and the total dataset (35 samples) (Table 3). No significant correlations were found with any of the parameters studied except for process length and summer SSS and summer σ_t for the Atlantic-Caribbean (Table 3). In addition, no significant correlation was found between the process length and cyst body diameter (R^2=0.02).

3.3.4. Cyst wall geochemistry

Three to six cysts from both biogeographic provinces showed consistent IR spectra; thus, representative spectra are shown (Fig. 8). In specimens from Indonesia (Ambon and Kao Bay), there were clear absorptions for: O-H stretching (~3250 cm^{-1}); C-H stretching (2912 and 2850 cm^{-1} (Ambon), 2908 and 2846 cm^{-1} (Kao Bay)); ring stretching (1590 cm^{-1}); C-H and ring bending (1361 and 1350 cm^{-1} (Ambon), 1365 and 1353 cm^{-1} (Kao Bay)). There were also several absorptions between 1160-1000 cm^{-1}, including the strongest ones at 1041 cm^{-1} (Ambon) and 1037 cm^{-1} (Kao Bay). These indicated stretching vibrations (C-C, C-O, C-O-C) associated with polysaccharides (e.g., Kačuráková et al., 2002). There were also absorptions at 985 cm^{-1} (O-CH_3 of polysaccharides) and in the Ambon specimens, at 760 cm^{-1} (C-H out-of-plane bending).

In general, the Ambon residue was visually cleaner than the Kao Bay residue prior to treatment. Abundant bacteria were observed in the Kao Bay residue and, while they were gone after processing, it is possible some extraneous material was still present on the cyst walls. This could explain the shoulders at 1630 cm^{-1}, 1535 cm^{-1} and 1250 cm^{-1}, which suggest contamination. Nevertheless, the overall similarity between Ambon and Kao Bay spectra contrast with specimens from Florida, USA (West Lake). In those spectra, there were many of the same absorptions found in the Indonesian spectra (Fig. 8), including the absorption series (1160-1000 cm^{-1}) that is indicative of polysaccharides. However, the strongest stretching absorption between 1160-1000 cm^{-1} was positioned at 1010 cm^{-1}. This is significant as it suggests a different polysaccharide is more abundant in the cyst wall. This is further supported by the absorptions at 1618 cm^{-1}, which were lacking in the Indonesian specimens, and at 972 cm^{-1} ($O-CH_3$ of polysaccharides). Both of these are typically found in the spectra of pectin (Schulz and Baranska, 2007). There was also an additional absorption at 1730 cm^{-1} (carbonyl stretching) that, together with stronger aliphatic C-H stretching (2915 and 2850 cm^{-1}), imply that Indo-Pacific specimens have a greater abundance of fatty acid esters in the cyst wall. Other differences included bending vibrations (1440 cm^{-1}, 1407 cm^{-1} and 1311 cm^{-1}) that are shifted from those found in the Indonesian spectra.

3.4. Molecular phylogenetic analysis

A phylogenetic tree based on LSU rDNA, was constructed by including other species belonging to the order Gonyaulacales. We examined the phylogenetic relationship among several strains of *P. bahamense*: two strains from the Philippines, one strain from Puerto Rico, three strains from Florida, six strains from Oyster Bay (Jamaica) and included the reported sequences by Ellegaard et al. (2003) and Leaw et al. (2005), as well as other Gonyaulacales (Fig. 9). On the ML tree of LSU rDNA, a clade consisting of all sequenced *Pyrodinium bahamense* strains was located close to, but independent from, the clade of *Alexandrium* (Figs. 7, 9). Within the former clade, two sub-clades are observed, one containing the Indo-Pacific strains and the other containing the Atlantic-Caribbean strains. Our results showed no significant genetic distance within the Indo-Pacific strains and within the Atlantic-Caribbean strains (0.000%), but a short distance was found between the Indo-Pacific and the Atlantic-Caribbean strains (0.012%). This distance is very short in comparison to the distances between the *Pyrodinium bahamense* strains and the *Alexandrium* species (between

0.345 and 0.807%). No hybrids were observed: in 659 bp of the LSU, only three bp are different at positions 55 (C:T), 94(A:C) and 170 (T:C) and these differences are concordant with both ribotypes.

4. Discussion

Here we discuss whether specimens from the Indo-Pacific can be unambiguously separated from specimens from the Atlantic-Caribbean, using the morphology of motile stage and cyst (4.1), cyst wall chemistry (4.2) and nuclear rDNA (4.3). Subsequently, we review how these observations conform to the biogeography (4.4) and capability of PSP production (4.5). In addition we discuss the importance of life cycle stages in relation to the morphological variation (4.6).

4. 1. Morphological characteristics of *Pyrodinium bahamense*

4.1.1. Motile stage

The results show that the variability in body length and the morphological characteristics of Steidinger et al. (1980), *in casu*, the ability to form chains, the anterior-posterior compression, the presence of a broad apical horn and the lack of an antapical spine and list system, the size of the trichocyst pores and the presence of 4 to 5 apical plates do not allow unambiguous differentiation of var. *compressum* from var. *bahamense*. These results support previous morphological observations of the vegetative stage by Balech (1985). Balech (1985) carefully observed the morphology of *P. bahamense* collected from Jamaica in the Atlantic and the Philippines in the Pacific and concluded that all morphological features intergrade.

4.1.2. Morphological differentiation of cyst forms

Previously, Matsuoka et al. (1989) suggested that Pacific cysts of *Pyrodinium bahamense*, which were considered to belong to var. *compressum*, have a larger body and relatively shorter processes than the cysts of *P. bahamense* var. *bahamense*. In this study, Atlantic-Caribbean specimens are on average slightly smaller in body size and bear slightly shorter processes than their counterparts from the Indo-Pacific. However, there was no unequivocal way to differentiate cysts from the two geographical areas using the morphology of the cyst. The comparison to the environmental data revealed that there were no significant correlations between salinity, temperature or density with body diameter and process length. However, at a regional scale, in the Atlantic Caribbean, a significant relationship can be established between the process length and summer sea surface salinity (and summer sea surface density) (summer sea surface salinity = 4.1964 * process length - 8.5774; R^2=0.88). This suggests that process length can be regulated by salinity variations, similar to what is suggested for other gonyaulacoid cysts, in particular *Lingulodinium machaerophorum* (Mertens et al., 2009) and the cysts of *Protoceratium reticulatum* (Mertens et al., 2011). The lack of a significant correlation between process length and salinity for the Indo-Pacific specimens may be due to the narrow salinity range at regional scale and lack of modern analogues representing low salinities. It seems likely that cyst body diameter is regulated by environmental parameters other than salinity and temperature, such as nutrients or turbulence.

4.2. Differences in cyst wall chemistry

The consistent differences between the cyst wall spectra from the Indo-Pacific and the Atlantic-Caribbean are surprising. All of the spectra suggest a cyst wall made primarily from polysaccharides; however, all of the specimens show distinctions to previously published gonyaulacoid spectra (Versteegh et al., 2012; Bogus et al., 2014), furthering the assertion in Bogus et al. (2014) that different sugar compounds are likely in dinoflagellate cyst walls. Of particular importance to this study is that the primary absorption in the polysaccharide stretching region indicates that a different polysaccharide is more abundant in the cyst walls of the Atlantic specimens. This variety exhibited numerous absorptions characteristic of pectins (linear (1-4)-linked α-D-galacturonan backbone with different side chains; Kačuráková and Wilson, 2001). That evidence, together with a higher presence of fatty acid esters in Atlantic specimens, indicates a different wall composition from the more aromatic Indo-Pacific specimens.

There are two possible explanations for these differences: (1) cysts from the two geographic regions build cyst walls with inherently different compositions and/or

(2) environmental and/or diagenetic factors have influenced the cyst wall composition. Given the molecular phylogenetic results that suggest a recent separation of the varieties (see section 4.3), it is not likely both types have had enough time, evolutionarily speaking, to alter their cyst wall compositions in a fundamental way. Taxon specific differences have been suggested in fossil species of one genus (Bogus et al., 2012); however, variability in modern species' cyst wall chemistry has recently been suggested to rely more on environmental factors than phylogeny (Bogus et al., 2014). The three samples were chosen because they originated from the biogeographic end-members, the Indo-Pacific and the Atlantic-Caribbean. As these bodies of water have different environmental parameters, it is more plausible that the cyst wall chemical differences are due to environmental variations. Differences in the environment could lead to a different biochemistry within the dinoflagellate (Geider and La Roche, 2002; Fuentes-Grünewald et al., 2009, 2012) and may affect the cyst wall composition, which could also be related to the differences observed in the morphology.

4.3. Molecular phylogenetic analysis

Leaw et al. (2005) carried out a phylogenetic analysis focusing on the genera *Alexandrium* and *Pyrodinium* in the Gonyaulacales based on LSU rDNA sequences and morphological characteristics using the specimens that they considered identical to *P. bahamens*e var. *compressum* collected from Sabah, Malaysia. They found that var. *compressum* is nested within the *Alexandrium* clade and particularly the clade consisting of *Alexandrium pseudogonyaulax* and *A. taylori*. This study represents the first published molecular comparison between *P. bahamense* isolates from the Atlantic-Caribbean and Indo-Pacific. On the ML tree of LSU rDNA, the *Pyrodinium* clade was independent from the *Alexandrium* clade (Fig. 7). Within the *Pyrodinium* clade, strains from the Indo-Pacific and Atlantic-Caribbean strains formed two distinct ribotypes that were well-separated by a short genetic distance (0.012%), suggesting a separation that occurred during the late Quaternary, i.e., on a millennial scale. However, the most plausible mechanism that would explain the separation is the closure of the Panama Isthmus around ~2.5 Ma and the associated changes in oceanic circulation (e.g., Schmidt, 2007), but this event occurred long before the late Quaternary. Further genetic work will hopefully resolve this discrepancy.

4.4. Biogeography

The biogeography of the two varieties was initially thought to be well-separated. *P. bahamense* var. *compressum* was considered endemic to the Indo-Pacific, while var. *bahamense* occurred in the Atlantic-Caribbean. This view is now known to be incorrect because of the co-occurrence of both varieties in the Persian Gulf (Al-Muftah, 1991; Glibert et al., 2002), Costa Rica (Vargas-Montero and Freer, 2003), the Gulf of California (Morquecho, 2008) and the Pacific coast of Mexico (Gárate-Lizzárraga and González-Armas, 2011).

4.5. Capability of PSP-toxin production

Steidinger et al (1980) listed six principal differences between the *Pyrodinium bahamense* varieties. One of the differences named was the ability to produce a toxin. Historically, *P. bahamense* var. *compressum* was known to be a saxitoxin producer (MacLean, 1973; Worth et al., 1975; Beales, 1976), while *P. bahamense* var. *bahamense* was known for not producing saxitoxin or at least not causing PSP intoxication (Steidinger et al., 1980). However, beginning in 2002, saxitoxin was detected in puffer fish harvested from the Indian River Lagoon (Florida, USA), which coincided with a *P. bahamense* var. *bahamense* bloom. Cultures established from these bloom waters demonstrated the ability to produce saxitoxin (Landsberg et al., 2006). The discovery that Indian River Lagoon populations of *P. bahamense* var. *bahamense* produced toxins spurred researchers in Florida to examine other areas for the presence of saxitoxin in water and pufferfish tissues. Abbott et al. (2009) reported finding saxitoxin in seven other Florida estuaries, including Tampa Bay, where *P. bahamense* var. *bahamense* populations were examined by Steidinger et al. (1980) and morphologically in this study. Cultures developed from Tampa Bay isolates also produce saxitoxin (FWRI, unpublished data).

Even though monitoring efforts for saxitoxin in Florida continue, more work is needed to determine the toxin-producing potential of other Atlantic and Caribbean-based populations of *P. bahamense* var. *bahamense*. As suggested by Usup et al. (2012), it would be advantageous to study isolates of the Pacific Ocean type to help determine if these strains are weakly toxic and thus only become a health concern through bioaccumulation or under certain environmental conditions. In any case and most relevant to this study is that the ability to produce toxins is not a useful characteristic to separate the varieties.

4.6. The relation between the life cycle and morphological variation

Our observations of cells from diverse locations (Table 1) have shown us that specimens that can be assigned to both "varieties" and may be present in the same plankton sample. As we mentioned earlier, both varieties have previously been reported to co-occur in several locations such as Costa Rica (Vargas-Montero and Freer, 2003), the Pacific coast of Mexico (Gárate-Lizárraga and González-Armas, 2011) and the Arabian Gulf (Glibert et al., 2002). Instead of varieties, they are most likely, developmental stages in the life cycle of *Pyrodinium bahamense* (Suppl. plate 1-6) as we explain below.

The earliest studies of the life cycle of *Pyrodinium bahamense* only included a vegetative phase. The first one, by Buchanan (1968) and the second one, carried out almost simultaneously, by Wall and Dale (1969) showed comparable results. Unfortunately, the observations were registered as light microscope images, which show little detail of the thecal plates. Usup and Azanza (1998) described the life cycle but provided no detailed descriptions or photographs. The more recent studies on the germination of cysts of *P bahamense* (e.g., Badylak and Phlips, 2009; Morquecho et al., 2014) have not expanded our knowledge on the life cycles of *Pyrodinium bahamense.* One thing is clear: none of the large cells that we have observed in this study have been observed by those authors. These large cells, with very wide growth bands, probably belong to a different stage of the life cycle of *Pyrodinium bahamense,* a sexual stage that has not been observed yet (e.g., Plate 7A-D,F, Suppl. Plate 1). We suggest that such large cells may be planozygotes (and possible planomeiocytes), which would be in accordance with planozygotes observed for other species (e.g., Pfiester and Anderson, 1987), especially in the closely related genus *Alexandrium* (*A. catenella* (Uribe et al., 2010) and *A. fundyense* (McGillicuddy et al., 2014).

The apical pore complex varied between two end-members: a small cell with a less developed apical and antapical lists/spines, pore plate (PO) with a broad margin, a narrower cover plate (PI) with sparse ornamentation, no growth bands, an elongated apical attachment pore on the PO, an antapical attachment pore on the posterior sulcal plate, fewer pores with smaller diameters and a large cell with well-developed apical and antapical lists/spines, a PO with a narrow margin, a wider PI with more intricate ornamentation, growth bands, no apical attachment pore on the PO, no antapical attachment pore on the posterior sulcal plate, more pores with larger diameters (Plates 1, 3-4).

Schematics of the general sexual life cycle of dinoflagellates have been summarized in detailed by Pfiester (1984, her Fig. 1, p. 184) and Pfiester and Anderson (1987, their Fig. 14-10, p. 626). There was a tremendous variety of cells of *Pyrodinium bahamense* found in this study, and at this point, without having followed its complete life cycle, we could not say with certainty which cells correspond to the vegetative cells, gametes or planozygotes (or planomeiocytes). There was variation not only in the body size, but also in size and number pores on the thecal plates, as well as the development of the apical and antapical lists and growth bands, absence or presence of apical and antapical spines or of anterior and posterior attachment pores. Since it has been suggested that dinoflagellate gametes actually look similar to the vegetative cells, only much smaller (Pfiester 1984), we might attribute some of the observed cells to be gametes (Plate 6B, C). These cells have the apical and antapical lists/spines well developed, but they do not exhibit the growth bands that larger cells with developed list/spines do, which potentially represent the planozygotes (Plate 4C). Flow cytometry technology, such as that developed by McGillicuddy et al. (2012) may be useful to establish the proportion of *P. bahamense* populations that are gametes, vegetative cells, and planozygotes which could help explain the morphological variation observed here.

5. Conclusions

Based on our investigation of both theca and cyst morphological features, as well as what is known about the biogeographic distribution and capacity of PSP toxin production, *Pyrodinium bahamense* var. *bahamense* and *P. bahamense* var. *compressum* cannot be unequivocally separated using the original defining morphological characteristics, range or toxicity. We therefore recommend ceasing to use these varieties (and forma). Additionally, we suggest that observations of both varieties in a single plankton sample should be interpreted as different life stages in such samples. However, in a phylogenetic analysis using LSU rDNA showed that the strains fall into Indo-Pacific and Atlantic-Caribbean ribotypes, separated by a short genetic distance, which suggests a separation that occurred in the late Quaternary. It is of interest that geochemical analyses of the cyst wall also show differences between both regions, although this finding is more likely related to environmental factors than an evolutionary separation. Given the morphological continuity, it is not clear whether the two ribotypes correspond to the original delineation of the two varieties. Both ribotypes should be further investigated by mating and life cycle studies in combination with molecular and toxicology studies using isolates from both geographic provinces.

Acknowledgements

David Wall and Lucy E. Edwards are thanked for the use of slides. We would like to thank Warner Brückmann and Silke Schenk (IFM Geomar) for sampling the core from the Red Sea and we acknowledge the Scripps Institution of Oceanography (SIO) Geological Collections and in particular Alex Hangsterfer for sediment samples from the Bay of Bengal. We are grateful to Theodore Smayda for providing the plankton sample from Oyster Bay (Jamaica). We appreciate help from Martin J. Head with the interpretation of the paratabulation on the cysts. Andreas Kronenberg is thanked for the use of the micro-FTIR spectrometer. Matthew Garrett and Bill Richardson (FWRI) are thanked for their assistance with sampling and culturing. Maryse Henry and Rayland Lapointe are acknowledged for help with SEM preparations at GEOTOP. Cecilia Puchulutegui (FWRI) is gratefully acknowledged for providing sequences, and Mitsunori Iwataki and Hisae Kawami for help with sequencing. Constructive comments of anonymous reviewers are greatly appreciated.

References

Abbott, J., Flewelling, L., Landsberg, J., 2009. Saxitoxin monitoring in three species of Florida puffer fish. Harmful Algae 8, 343–348.

Al-Muftah, A.R., 1991. Dinoflagellates of Qatari Waters. PhD thesis. University College of North Wales, Bangor University, 261 pp., 2 Vol.

Badylak, S., Kelley, K., Phlips, E.J., 2004. A description of *Pyrodinium bahamense* (Dinophyceae) from the Indian River Lagoon, Florida, US. Phycologia 43, 653–657.

Badylak, S., Phlips, E.J., 2009. Observations of multiple life stages of the toxic dinoflagellate *Pyrodinium bahamense* (Dinophyceae) in the St. Lucie estuary, Florida. Fla. Sci. 72, 208–217

Balech, E., 1985. A redescription of *Pyrodinium bahamense* Plate (Dinoflagellata). Rev. Palaeobot. Palynol. 45, 17–34.

Beales, R., 1976. A red tide in Brunei's coastal waters. Brunei Mus. J. 3, 167–182.

Bogus, K., Harding, I.C., King, A., Charles, A.K., Zonneveld, K., Versteegh, G.J.M. 2012. The composition of species of the *Apectodinium* complex (Dinoflagellata). Rev. Palaeobot. Palynol. 183, 21–31.

Bogus, K., Mertens, K.N.M., Lauwaert, J., Harding, I.C., Vrielinck, H., Zonneveld, K., Versteegh, G.J.M., 2014. Differences in the chemical composition of organic-walled dinoflagellate resting cysts from phototrophic and heterotrophic dinoflagellates. J. Phycol. 50, 254–266.

Böhm, A., 1931. Peridineen aus dem Persischen Golf und dem Golf von Oman. Arch. Protistenkd. 74, 188–197.

Buchanan, R.J., 1968. Studies at Oyster Bay in Jamaica, West Indies. IV, Observations on the morphology and a sexual cycle of *Pyrodinium bahamense* Plate. J. Phycol. 4, 272–277.

Colthup, N.B., Daly, L.H., Wiberly, S.E., 1990. Introduction to Infrared and Raman Spectroscopy. Academic Press Limited, London, 282 pp.

Conkright M.E., Locarnini, R.A., Garcia, H.E., O'Brien, T.D., Boyer, T.P., Stephens, C., Antonov, J.I., 2002. World Ocean Atlas 2001: Objective Analyses, Data Statistics, and Figures, CD-ROM Documentation. National Oceanographic Data Center, Silver Spring, MD, 17 pp.

Ellegaard M., Daugbjerg, N., Rochon, A., Lewis, J., Harding, I., 2003. Morphological and LSU rDNA sequence variation within the *Gonyaulax spinifera*-*Spiniferites* group (Dinophyceae) and proposal of *G. elongata* comb. nov. and *G. membranancea* comb. nov.. Phycologia 42, 151–164.

Felsenstein, J., 1985. Confidence limits on phylogenies: An approach using the bootstrap. Evolution 39, 783–791.

Fensome, R. A., Taylor, F.J.R., Norris, G., Sarjeant, W.A.S., Wharton, D.I., Williams, G.L. 1993. A classification of living and fossil dinoflagellates. Micropaleontology, Special Publication 7, 1–351.

Fuentes-Grünewald, C., Garcés, E., Rossi, S., Camp, J. 2009. Use of the dinoflagellate *Karlodinium veneficum* as a sustainable source of biodiesel production. J. Ind. Microbiol. Biotechnol. 36: 1215–1224.

Fuentes-Grünewald, C., Garcés, E., Alacid, E., Sampedro, N., Rossi, S., Camp, J., 2012. Improvement in lipid production in the marine strains *Alexandrium minutum* and *Heterosigma akashiwo* by utilizing abiotic parameters. J. Ind. Microbiol. Biotechnol. 39, 207–216.

Gárate-Lizárraga, I., González-Armas, R., 2011. Occurrence of *Pyrodinium bahamense* var. *compressum* along the southern coast of the Baja California Peninsula. Mar. Pollut. Bull. 62, 626–630.

Geider, R., La Roche, J., 2002. Redfield revisited: variability of C:N:P in marine microalgae and its biochemical basis. Eur. J. Phycol. 37, 1–17.

Glibert, P.M., Landsberg, J.H., Evans, J.J., Al-Sarawi, M.A., Faraj, M., Al-Jarallah, A., Haywood, A., Ibrahem, S., Klesius, P., Powell, C., Shoemaker, C., 2002. A fish kill of massive proportion in Kuwait Bay, Arabian Gulf, 2001: the roles of bacterial disease, harmful algae and eutrophication. Harmful Algae 1, 215–231.

Gonzales, C.L., 1989. *Pyrodinium* blooms and paralytic shellfish poisoning in the Philippines. In: Hallegraeff, G.M., Maclean, J.L. (Eds.), Biology, epidemiology and management of *Pyrodinium* red tides. ICLARM Conference Proceedings 21, Fisheries Department, Ministry of Development, Brunei Darussalam, and International Center for Living Aquatic Resources Management, Manila, Philippines, p. 39–47.

Iwataki, M., Kawami, H., Matsuoka, K. 2007. *Cochlodinium fulvescens* sp. nov. (Gymnodiniales, Dinophyceae), a new chain-forming unarmored dinoflagellate from Asian coasts. Phycological Research 55, 231–239.

Jaafar, M.H., De Silva, M.W.R.N., Sharifuddin P.H.Y., 1989. *Pyrodinium* red tide occurrences in Brunei Darussalam. In: Hallegraeff, G.M., Maclean, J.L. (Eds.), Biology, epidemiology and management of *Pyrodinium* red tides. ICLARM Conference Proceedings 21, Fisheries Department, Ministry of

Development, Brunei Darussalam, and International Center for Living Aquatic Resources Managrnaent, Manila, Philippines, p. 9–17.

Kačuráková, M., Wilson, R.H., 2001. Developments in mid-infrared FT-IR spectroscopy of selected carbohydrates. Carbohyd. Polym. 44, 291–303.

Kačuráková, M., Smith, A.C., Gidley, M.J., Wilson, R.H., 2002. Molecular interactions in bacterial cellulose composites studied by 1D FT-IR and dynamic 2D FT-IR spectroscopy. Carbohyd. Res. 337, 1145–1153.

Kofoid, C.A., 1909. On *Peridinium steini* Jörgensen, with a note on the nomenclature of the skeleton of the Peridinidae. Arch. Protistenkd. 16, 25-47 + pl. II.

Kokinos, J.P., Anderson, D.M., 1995. Morphological development of resting cysts in cultures of the marine dinoflagellate *Lingulodinium polyedrum* (=*L. machaerophorum*). Palynology 19, 143–166.

Landsberg, J.H., Sherwood, H., Johannessen, J.N., White, K.D., Conrad, S.M., Abbott, JP., Flewlling, L.J., Richardson, R.W., Dickey, R.W., Jester, E.L.E., Etheridge, S.M., Deeds, J.R., Van Dolah, F.M., Leifield, T.A., Zou, Y., Beaudry, C.G., Benner, R.A., Rogers, P.L., Scott, P.S., Kawabata, K., Wolny, J.L., Steidinger, K.A., 2006. Saxitoxin puffer fish poisoning in the United States, with the first report of *Pyrodinium bahamense* as the putative toxin source. Environ. Health Persp. 114, 1502–1507.

Leaw, P.L., Lim, P.T., Ng, B.K., Cheah, M.Y., Ahmad, A., Usup, G., 2005. Phylogenetic analysis of *Alexandrium* species and *Pyrodinium bahamense* (Dinophyceae) based on theca morphology and nuclear ribosomal gene sequence. Phycologia 44, 550–565.

Maclean, J.L., 1973. Red tide and paralytic shellfish poisoning in Papua New Guinea. Papua New Guinea Agr. 24, 131–138.

Maclean, J.L., 1989. Red tides in Papua New Guinea waters, p. 27-38. In: Hallegraeff, G.M., Maclean, J.L. (Eds.), Biology, epidemiology and management of *Pyrodinium* red tides. ICLARM Conference Proceedings 21, Fisheries Department, Ministry of Development, Brunei Darussalam, and International Center for Living Aquatic Resources Management, Manila, Philippines. 286 p.

Matsuoka, K., 1989. Morphological features of the cyst of *Pyrodinium bahamense* var. *compressum*. In: Hallegraeff, G.M., Maclean, J.L. (Eds.) Biology, epidemiology and management of Pyrodinium red tides. ICLARM Conference Proceedings 21. Fisheries Department, Ministry of Development, Brunei Darussalam, and International Center for Living Aquatic Resources Management, Manila, Philippines, pp. 219–229.

Matzenauer, L., 1933. Die Dinoflagellaten des Indischen Ozeans (Mit Ausnahme der Gattung *Ceratium*). Botanisches Archiv 35(4), 437–510.

McGillicuddy Jr., D.J., Townsend, D.W., Keafer, B.A., Thomas, M.A., Anderson, D.M., 2012. Georges Bank: A leaky incubator of *Alexandrium fundyense* blooms. Deep-sea Research II 103, 163-173.

Mertens, K.N., Ribeiro, S., Bouimetarhan, I., Caner, H., Combourieu-Nebout, N., Dale, B., de Vernal, A., Ellegaard, M., Filipova, M., Godhe, A., Grøsfjeld, K., Holzwarth, U., Kotthoff, U., Leroy, S., Londeix, L., Marret, F., Matsuoka, K., Mudie, P., Naudts, L., Peña-Manjarrez, J., Persson, A., Popescu, S., Sangiorgi, F., van der Meer, M., Vink, A., Zonneveld, K., Vercauteren, D., Vlassenbroeck, J., Louwye, S., 2009. Process length variation in cysts of a dinoflagellate, *Lingulodinium machaerophorum*, in surface sediments investigating its potential as salinity proxy. Mar. Micropaleontol. 70**,** 54–69.

Mertens, K.N., Dale, B., Ellegaard, M., Jansson, I.-M., Godhe, A., Kremp, A., Louwye, S. 2011. Process length variation in cysts of the dinoflagellate *Protoceratium reticulatum*, from surface sediments of the Baltic-Kattegat-Skagerrak estuarine system: a regional salinity proxy. Boreas 40 (2), 242–255.

Morquecho, L., 2008. Morphology of *Pyrodinium bahamense* Plate (Dinoflagellata) near Isla San José, Gulf of California, Mexico. Harmful Algae 7, 664–670.

Morquecho, L., Alonso-Rodríguez, R., Martínez-Tecuapacho, G.A., 2014. Cyst morphology, germination characteristics, and potential toxicity of *Pyrodinium bahamense* in the Gulf of California. Bot. Marina 57, 303-314.

Ogata, T., Ishimaru, T., Kodama, M. 1987. Effect of water temperature and light intensity on growth rate and toxicity change in *Protogonyaulax tamarensis*. Mar. Biol. 95, 217–220.

Osorio Tafall, B.F.O., 1942. Notas sobre algunas Dinoflagelados planctónicos marinos de México, con descripción de nuevas especies. Anales de la E.N. de Ciencias Biologicas 2, 435–447.

Pfiester, L.A., 1984. Sexual reproduction. In: Spector, D.L. (Ed.), Dinoflagellates.

Academic press, Orlando (FL), pp. 181-199.
Pfiester, L.A., Anderson, D.A., 1987. Dinoflagellate reproduction. In: Taylor, F.J.R., The Biology of Dinoflagellates. Blackwell scientific publication, Oxford, pp. 611-648.
Plate, L., 1906. *Pyrodinium bahamense*. g., n. sp. die Leucht-Peridninee des “Feuersees” von Nassau, Bahamas. Archiv fur Protistenkunde und Protozen-algen-tilze 7, 411–429.
Rosales-Loessener, F., 1989. The Guatemalan experiences with red tides and paralytic shellfish poisoning. In: Hallegraeff, G.M., Maclean, J.L. (Eds.), Biology, epidemiology and management of *Pyrodinium* red tides. ICLARM Conference Proceedings 21. Fisheries Department, Ministry of Development, Brunei Darussalam, and International Center for Living Aquatic Resources Management, Manila, Philippines, pp. 49–51.
Roy, R.N., 1977. Red tide and outbreak of paralytic shellfish poisoning in Sabah. Med. J. Malaysia 31, 247–251.
Schlitzer, R., 2012. Ocean Data View, http://odv.awi.de.
Schmidt, D.N., 2007. The closure history of the Central American seaway: evidence from isotopes and fossils to models and molecules. In: Williams, M., Haywood, A.M., Gregory, F J., Schmidt, D.N. (Eds), Deep-Time Perspectives on Climate Change: Marrying the Signal from Computer Models and Biological Proxies. The Micropalaeontological Society, Special Publications. The Geological Society, London, 429–444.
Scholin C.A., Herzog M., Sogin M., Anderson D.M., 1994. Identification of group and strain-specific genetic markers for globally distributed *Alexandrium* (Dinophyceae). II. Sequence analysis of a fragment of the LSU rRNA gene. J. Phycol. 30, 999–1011.
Schulz, H., Baranska, M., 2007. Identification and qualification of valuable plant substances by IR and Raman spectroscopy. Vibr. Spectrosc. 43, 13–25.
Steidinger, K., Tester, L.S., Taylor, F.J.R., 1980. A reconsideration of *Pyrodinium bahamense* var. *compressa* (Böhm) stat. nov. from Pacific red tides. Phycologia 19, 329–334.
Tamura K., Nei, M., Kumar S. 2004. Prospects for inferring very large phylogenies by using the neighbor-joining method. P. Nat. Acad. Sci. USA 101, 11030–

11035.

Tamura, K., Peterson, D., Peterson, N., Stecher, G., Nei, M., Kumar, S. 2011. MEGA 5* Molecular Evolutionary Genetics Analysis using Maximum Likelihood, Evolutionary Distance, and Maximum Parsimony Methods. Mol. Biol. Evol. 28, 2731–2739.

Taylor, F.J.R., 1976. Dinoflagellates from the International Indian Ocean Expedition. Bibliotheca Botanica 132, 1–234.

Taylor, F.J.R., Fukuyo, Y., 1989. Morphological features of the cell of *Pyrodinium bahamense.* In: Hallegraeff, G.M., Maclean, J.L. (Eds.), Biology, epidemiology and management of *Pyrodinium* red tides. ICLARM Conference Proceedings 21, Fisheries Department, Ministry of Development, Brunei Darussalam, and International Center for Living Aquatic Resources Management, Manila, Philippines, p. 207–217.

Uribe, J.C., Oyarzún, S., Latorre, V., 2010. *Alexandrium catenella* (Whedon & Kofoid) Balech, 1985, in Magellan waters, Chile. Anales Instituto Patagonia (Chile), 38, 103–110.

Usup, G., Azanza, R.V. 1998. Physiology and bloom dynamics of the tropical dinoflagellate *Pyrodinium bahamense*. In: Anderson D.M., Cembella, A.D, Hallegraeff, G.M. (Eds.), Physiological Ecology of Harmful Algal Blooms, NATA ASI Series, G41, pp. 81–94.

Usup, G., Ahmad, A., Matsuoka, K., Lim, P.T., Leaw, C.P., 2012. Biology, ecology and bloom dynamics of the toxic marine dinoflagellate *Pyrodinium bahamense.* Harmful Algae 14, 301–312.

Vargas-Montero, M., Freer, E., 2003. Co-occurrence of different morphotypes of *Pyrodinium bahamense* during an extensive bloom in Gulf of Nicoya, Costa Rica. In: Villalba, A., Reguera, B., Romalde, J.L., Beiras, R. (Eds.), Molluscan Shellfish Safety. Xunta de Galicia and IOC_UNESCO, pp. 211–217.

Versteegh, G.J.M., Blokker, P., Bogus, K., Harding, I.C., Lewis, J., Oltmanns, S., Rochon, A., Zonneveld, K.A.F., 2012. Flash pyrolysis and infrared spectroscopy of cultured and sediment derived *Lingulodinium polyedrum* (Dinoflagellata) cyst walls. Org. Geochem. 43, 92–102.

Wall, D., Dale, B., 1969. The "hystrichosphaerid" resting spore of the dinoflagellate

Pyrodinium bahamense, Plate, 1906. J. Phycol. 5, 140–149.

Wiadnyana, N.N., Sidabutar, T., Matsuoka, K., Ochi, T., Kodama, M., Fukuyo, Y., 1996. Note on the occurrence of *Pyrodinium bahamense* in eastern Indonesian waters. In: Yasumoto, T., Oshima, Y., Fukuyo, Y. (Eds.), *Harmful and Toxic Algal Blooms*. International Oceanographic Commission of UNESCO, pp. 53–56.

Worth, G.K., Maclean, J.L., Price, M.J., 1975. Paralytic shellfish poisoning in Papua New Guinea, 1972. Pac. Sci. 29, 1–5.

Figures

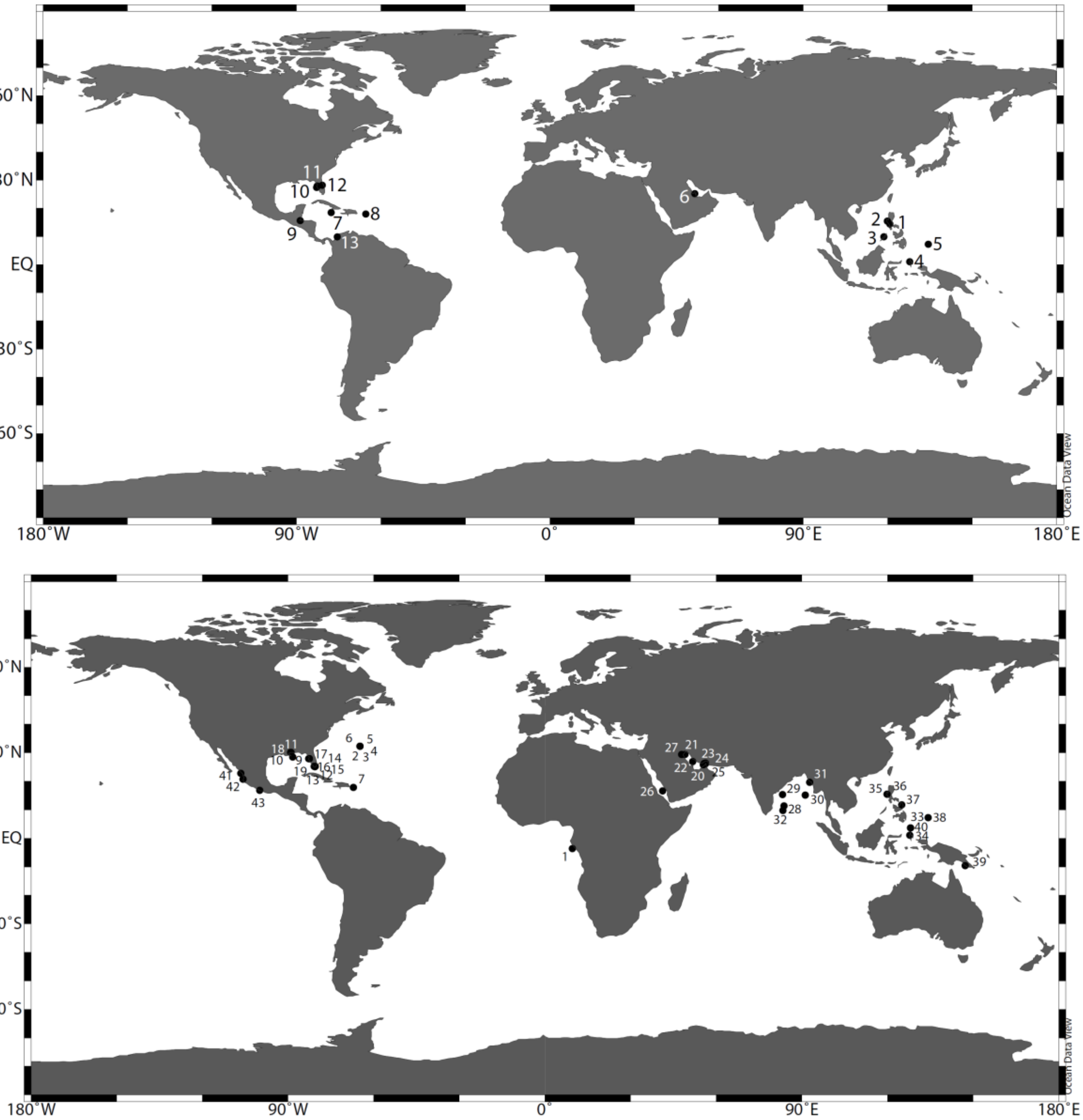

Fig. 1 Sampling locations of motile stage (A) and resting cysts (B) of *Pyrodinium bahamense* studied in the present study. Numbers on the maps correspond to numbers in Tables 1 and 2.

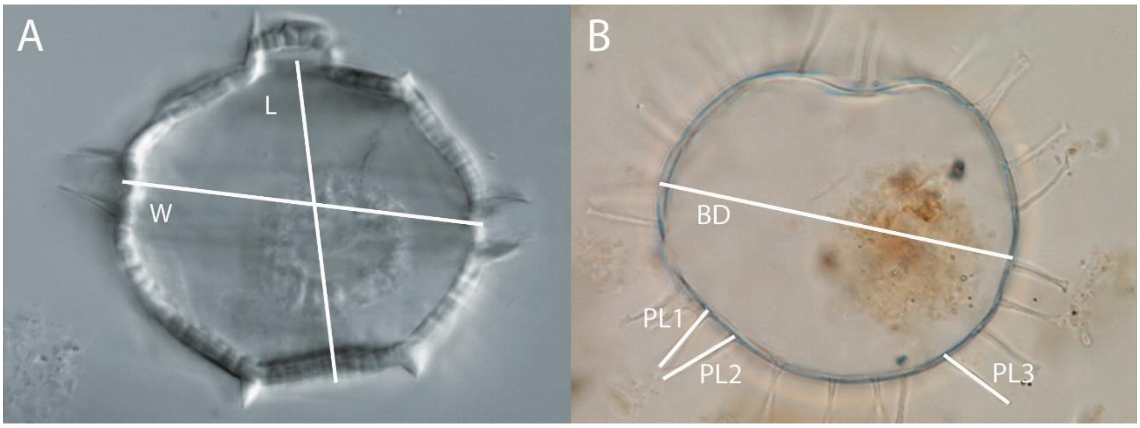

Fig. 2. (A) Measurement of body length (L) and body width (W) of the motile stage (specimen from Masinloc, the Philippines). (B) Measurement of largest body diameter (BD) and three process lengths of the cyst stage (PL1, PL2, PL3) (specimen from Bioluminescent Bay, Vieques, Puerto Rico).

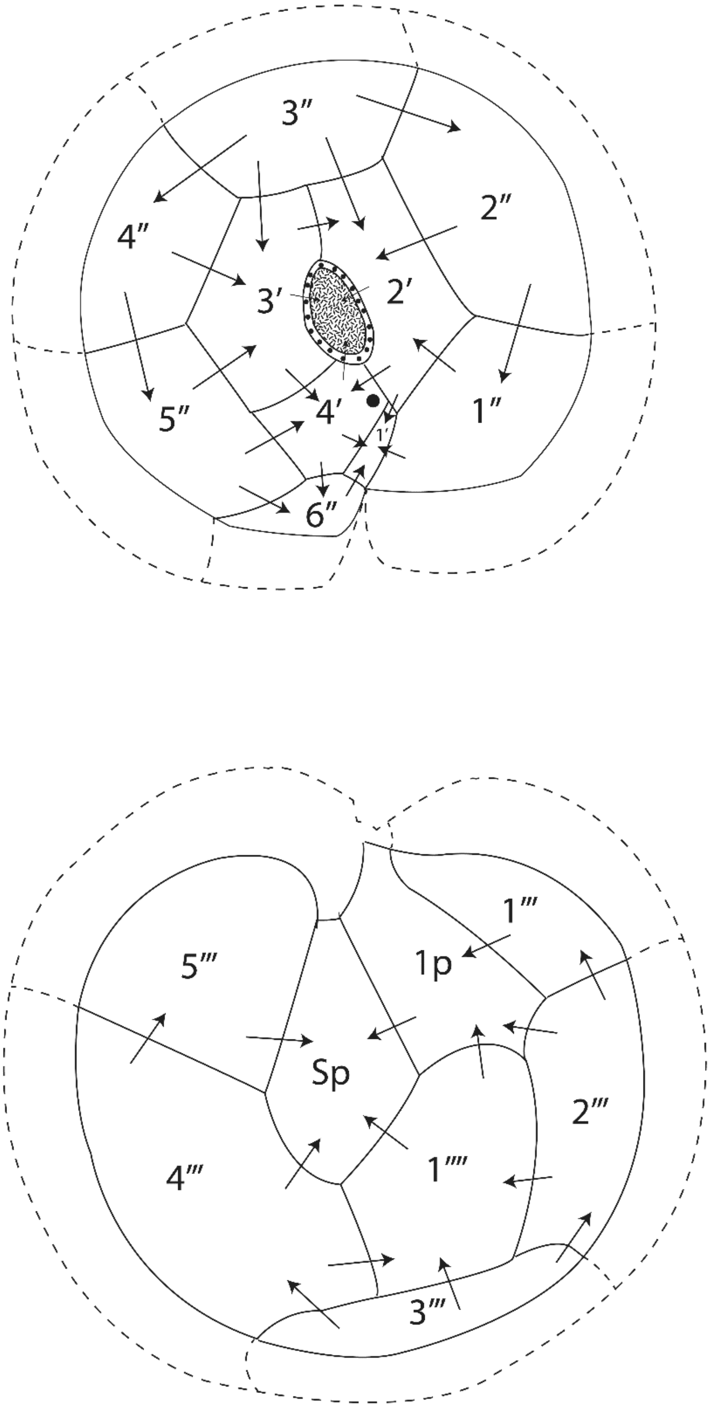

Fig. 3. Diagram showing the plate overlap in *Pyrodinium bahamense.* (A). Epitheca. Discontinued arrows point to plate names on the apical pore complex. (B). Hypotheca.

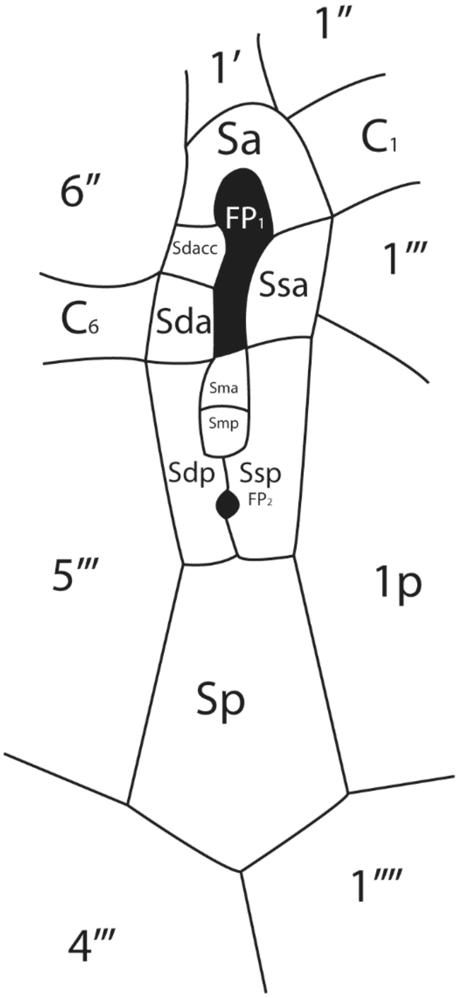

Fig. 4. Diagram showing the sulcal plates in *Pyrodinium bahamense* as observed under the scanning electron microscope. FP: flagellar pore; Sa: anterior sulcal plate; Sdacc: right anterior accessory sulcal plate (notation after Balech, 1985); Sda: right anterior sulcal plate; Sdp: right posterior sulcal plate; Sma: anterior medial sulcal plate; Smp: posterior medial sulcal plate; Ssa: anterior left sulcal plate (equivalent to 1‴ Kofoidean nomenclature, see text); Ssp: posterior left sulcal plate; Sp: posterior sulcal plate; C: cingular plates.

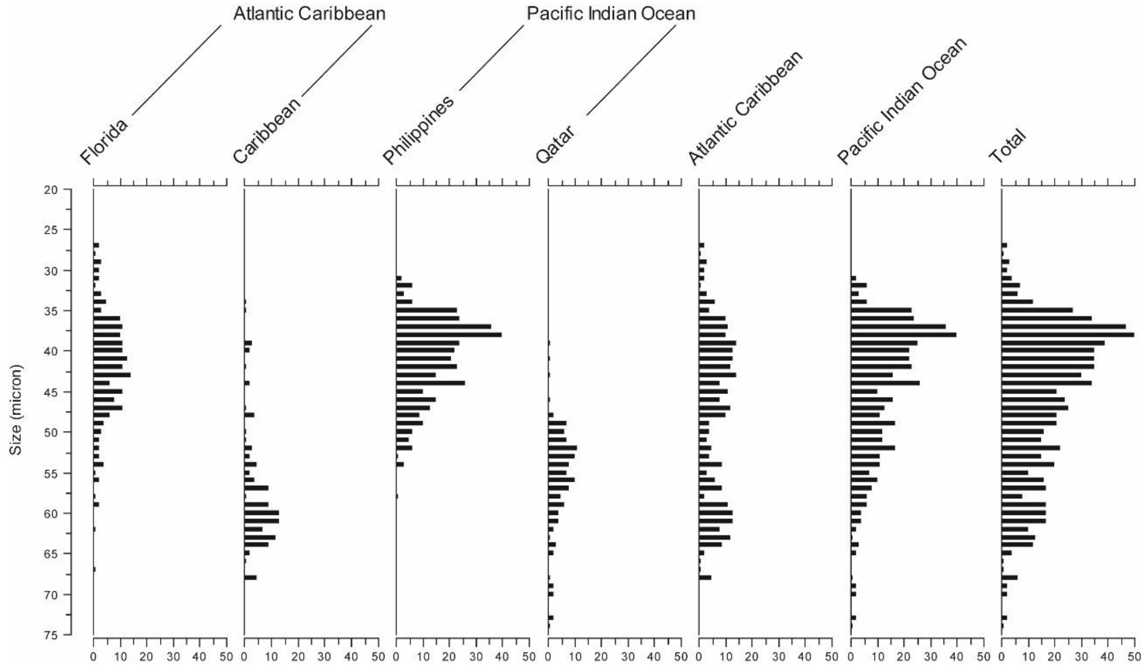

Fig. 5. Size-frequency curves of body length (L) of motile stage from Florida, Caribbean (combined as the Atlantic-Caribbean), the Philippines and Qatar (combined as Indo-Pacific) and the size-frequency spectrum of all measurements.

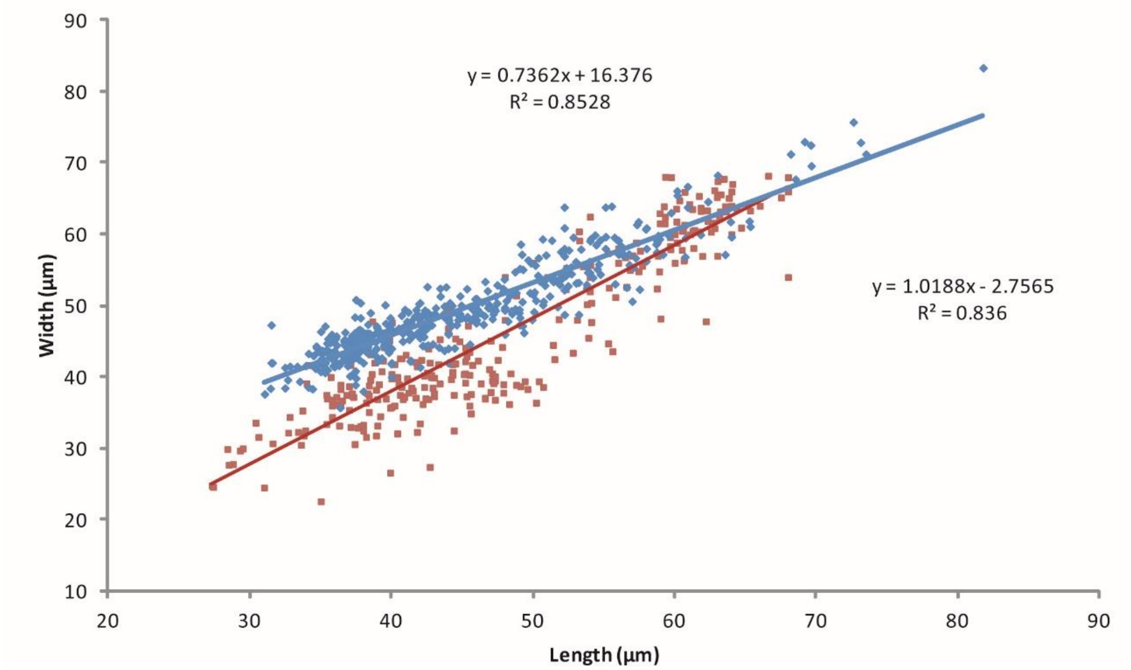

Fig. 6. Length-width diagram showing length (µm) and width (µm) of all measured thecae. The blue diamonds depicts specimens from the Indo-Pacific and the red squares

depict specimens from the Atlantic-Caribbean; note the strong overlap between both provinces.

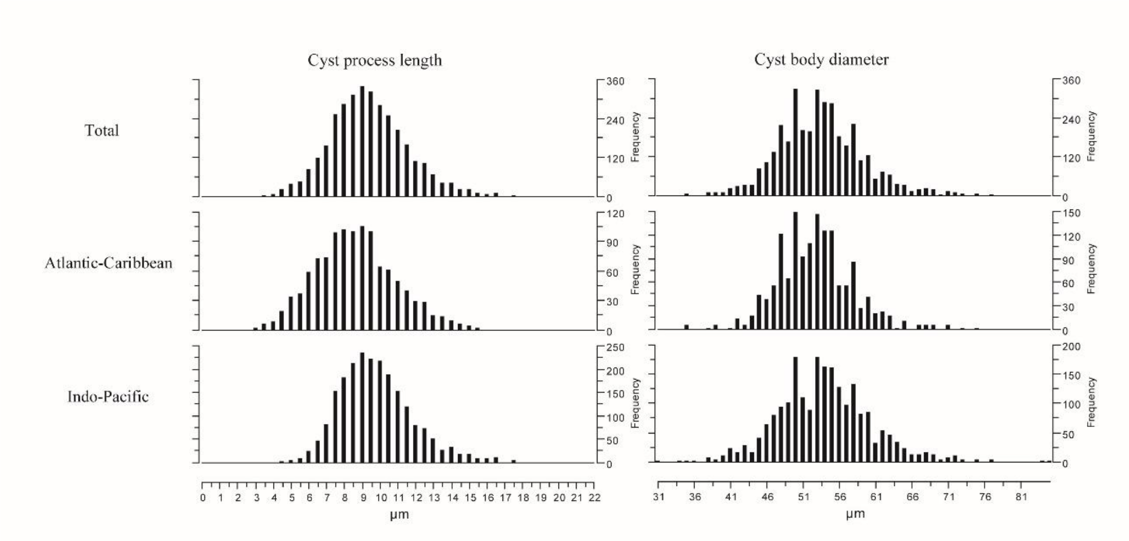

Fig. 7. Size-Frequency diagrams for cyst process length (left column) and cyst body diameter (right column) for the Indo-Pacific (lower row), Atlantic-Caribbean (middle row) and total dataset (upper row).

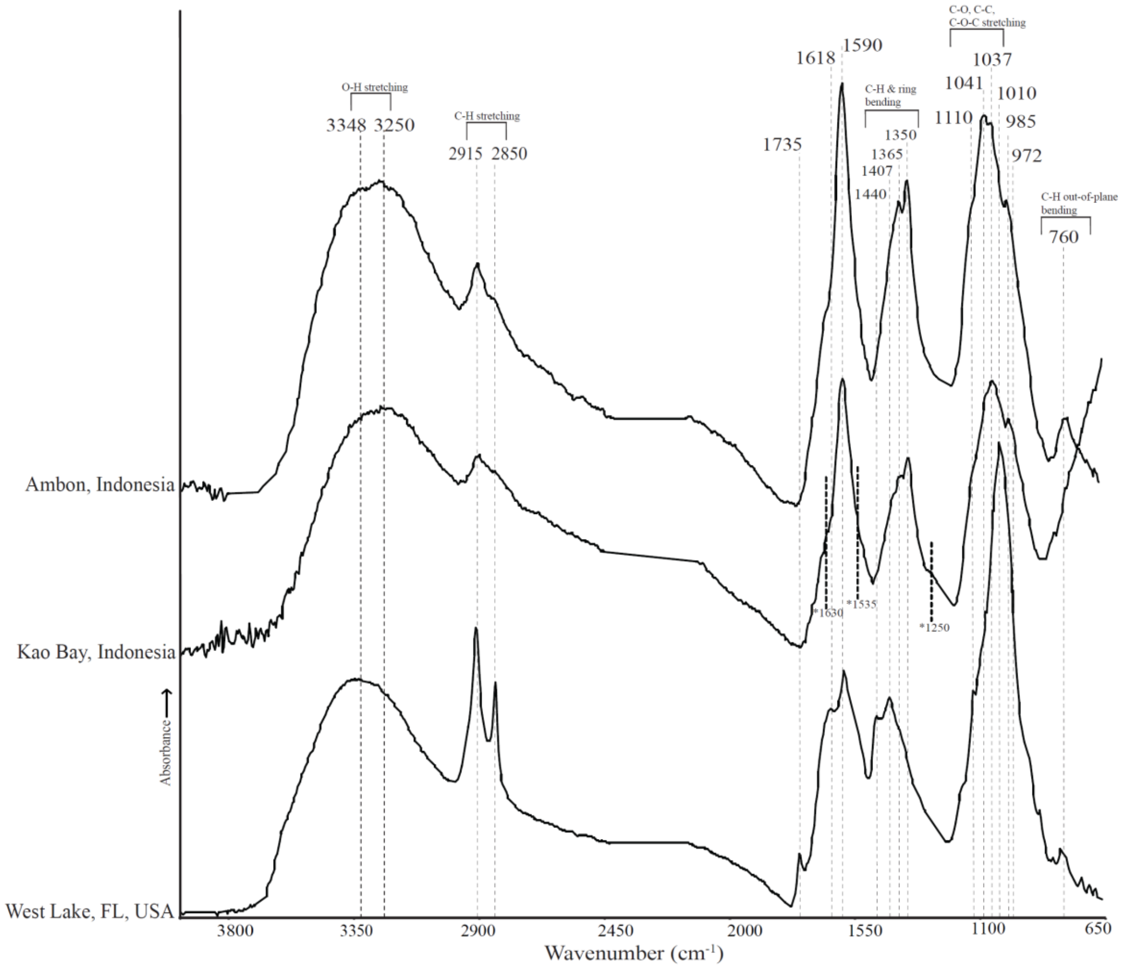

Fig. 8. Micro-FTIR spectra of representative cyst specimens of from Indonesia (Ambon and Kao Bay) and from the Atlantic (West Lake, FL, USA). For sample information, see Table 2 and Figure 1B. Asterisks (*) denote absorptions suggestive contamination, see text for details.

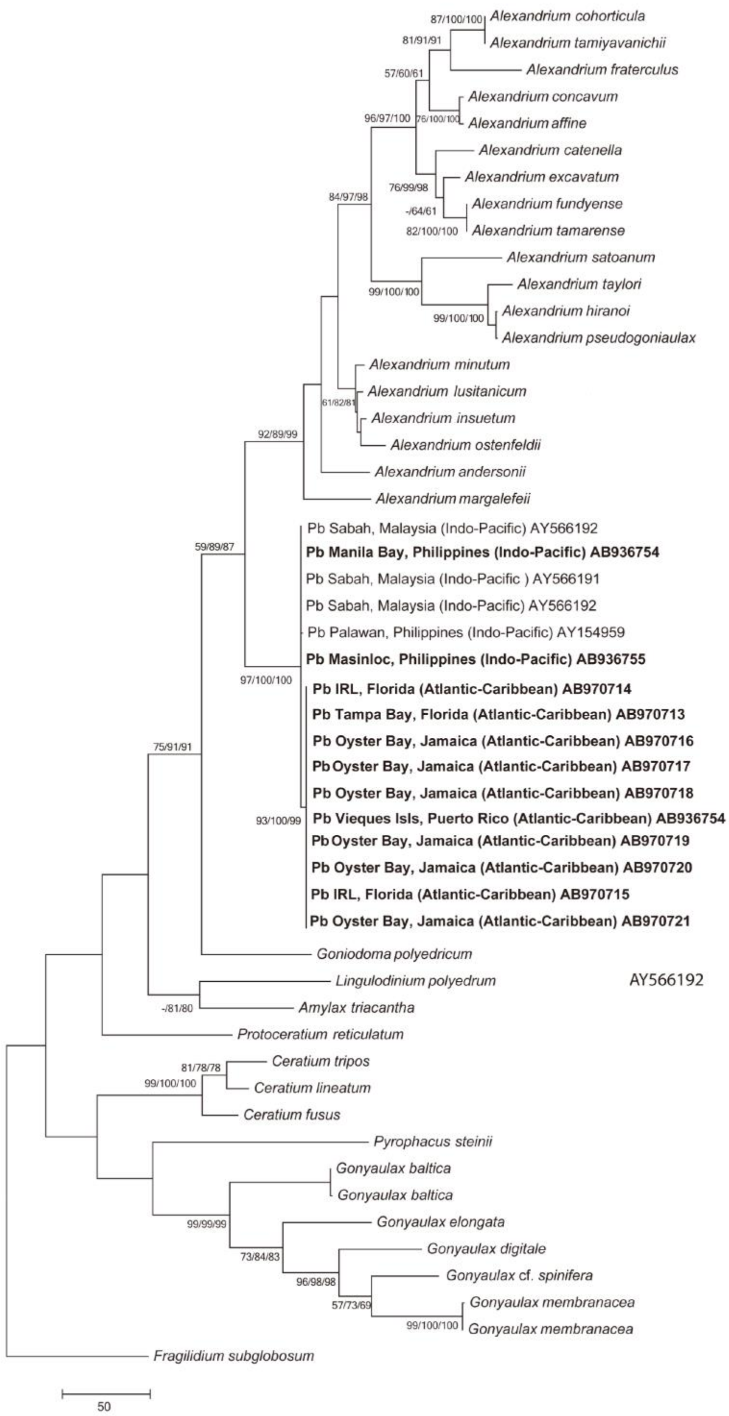

Fig. 9. Maximum likelihood tree constructed from LSU rDNA sequences using MEGA 5, showing phylogenetic relation between the Indo-Pacific morphotype and the Atlantic-Caribbean morphotype. Bootstrap percentages (>50%) for NJ/MP/ML methods are presented at each node. New sequences are shown in bold.

Plates

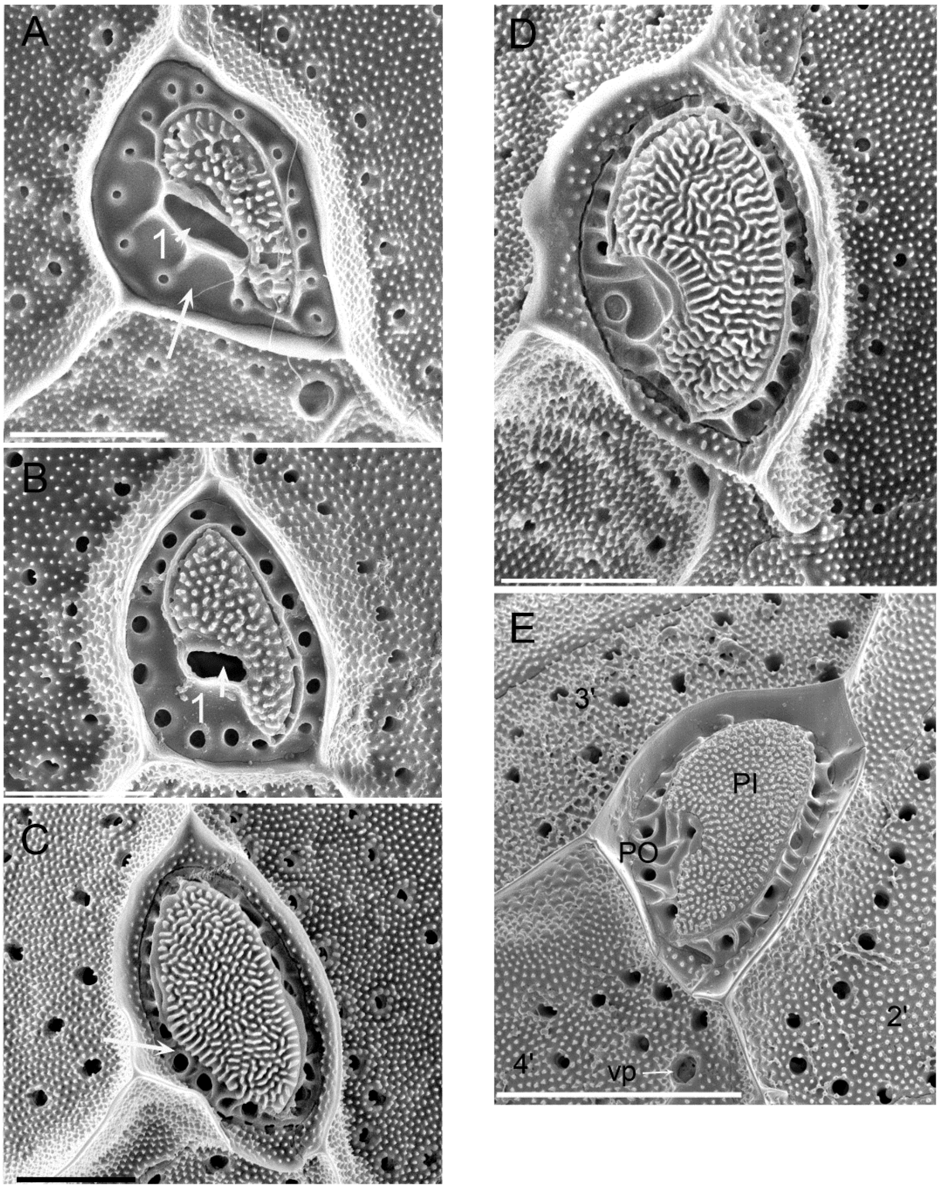

Plate 1. SEM photographs of *Pyrodinium bahamense* apical pore complex of cells listed in Table 1. (A). Cell from Bioluminescent Bay, Puerto Rico; long arrow denotes wide PO. (B). Cell from the Philippines (Masinloc Bay). (C). Cell from Bioluminescent Bay, Puerto Rico; long arrow denotes narrow PO. (D). Cell from Bioluminescent Bay, Puerto Rico. (E). Cell from Qatar. 1: Attachment pore; PI : cover or closing plate; PO: pore plate. Scale bars: 5 µm: A-D; 10 µm: E.

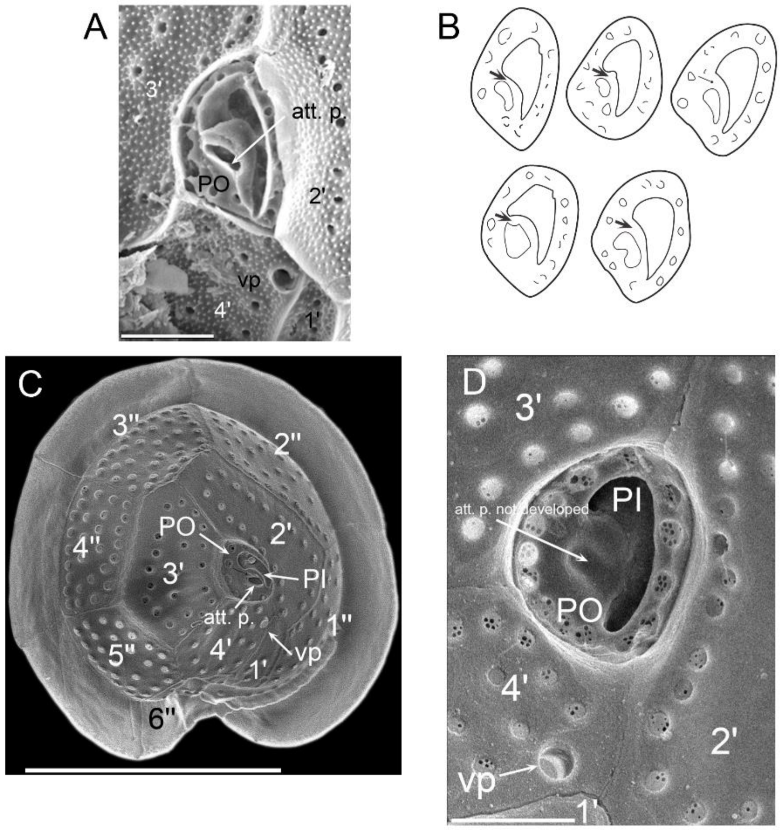

Plate 2. SEM photographs of *Pyrodinium bahamense* apical pore complex of cells listed in Table 1. (A). Cell from Bioluminescent Bay, Puerto Rico. Same cell of Plate 3e. Cover or closing plate missing. (B). Apical pores of cells from Papua New Guinea. Redrawn from Balech (1985, Pl. IV, Fig. 61). (C). Inside of an epitheca of a cell from the Philippines (San Pedro Bay). The original digital image has been flipped horizontally for easier visualization. (D). Inside of an epitheca of a cell from the Philippines (Masinloc Bay). Note that the attachment pore has not been developed yet. Also, compare the similarity of this inside of the apical pore complex with the outline of those shown in (C). Scale bars: 5 µm : A,D; 30 µm: D.

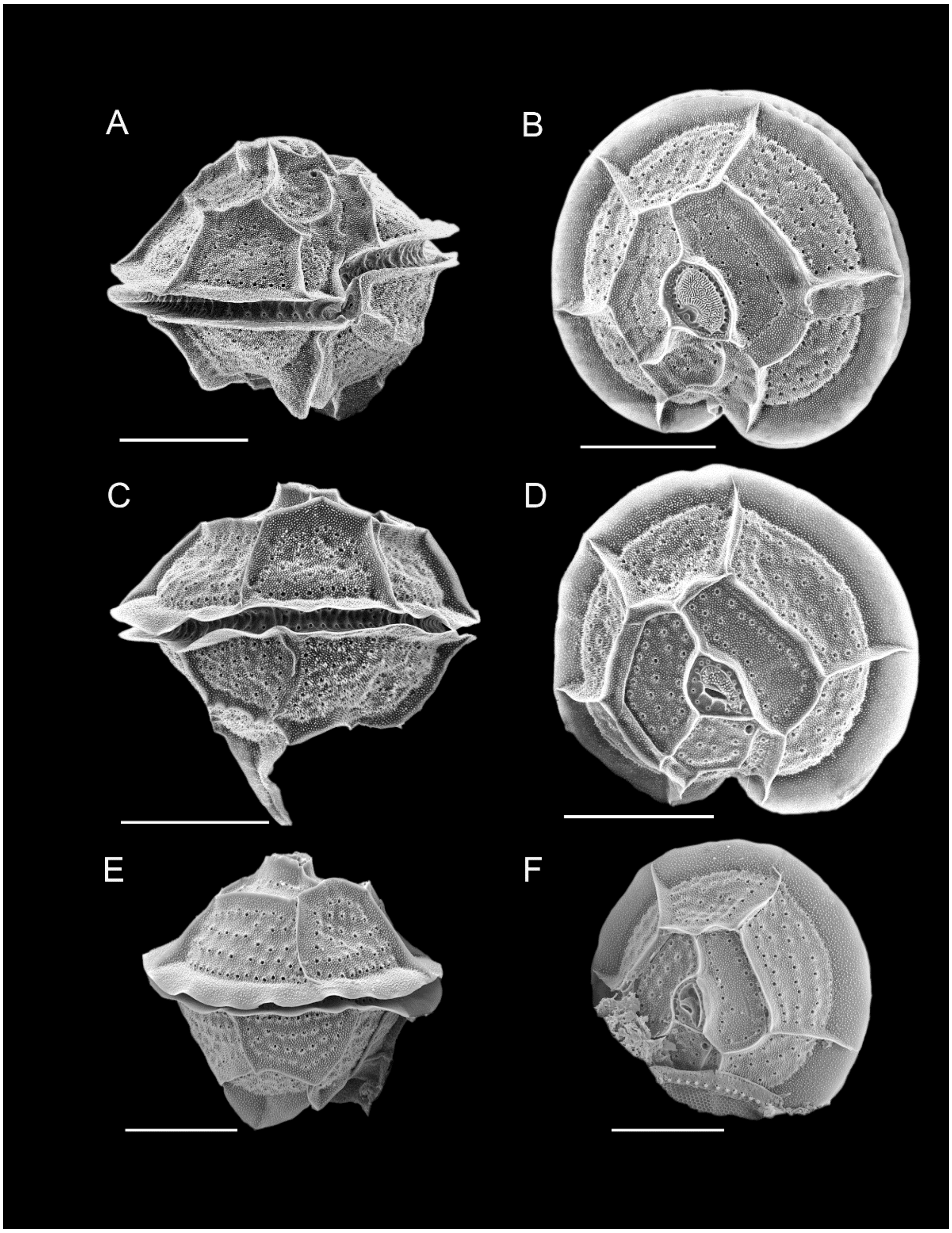

Plate 3. SEM photographs of *Pyrodinium bahamense* cells from Bioluminescent Bay (Puerto Rico), showing different developmental stages. Note the difference in thecal plate pore size and growth bands as well as list development. (A). Ventral view. (B). Apical view of cell shown in a. (C). Different cell. Right lateral view. (D). Apical view of cell shown in C. (E). Different cell. Right lateral view. (F). Apical view of cell shown in E. Scale bars: 20 µm.

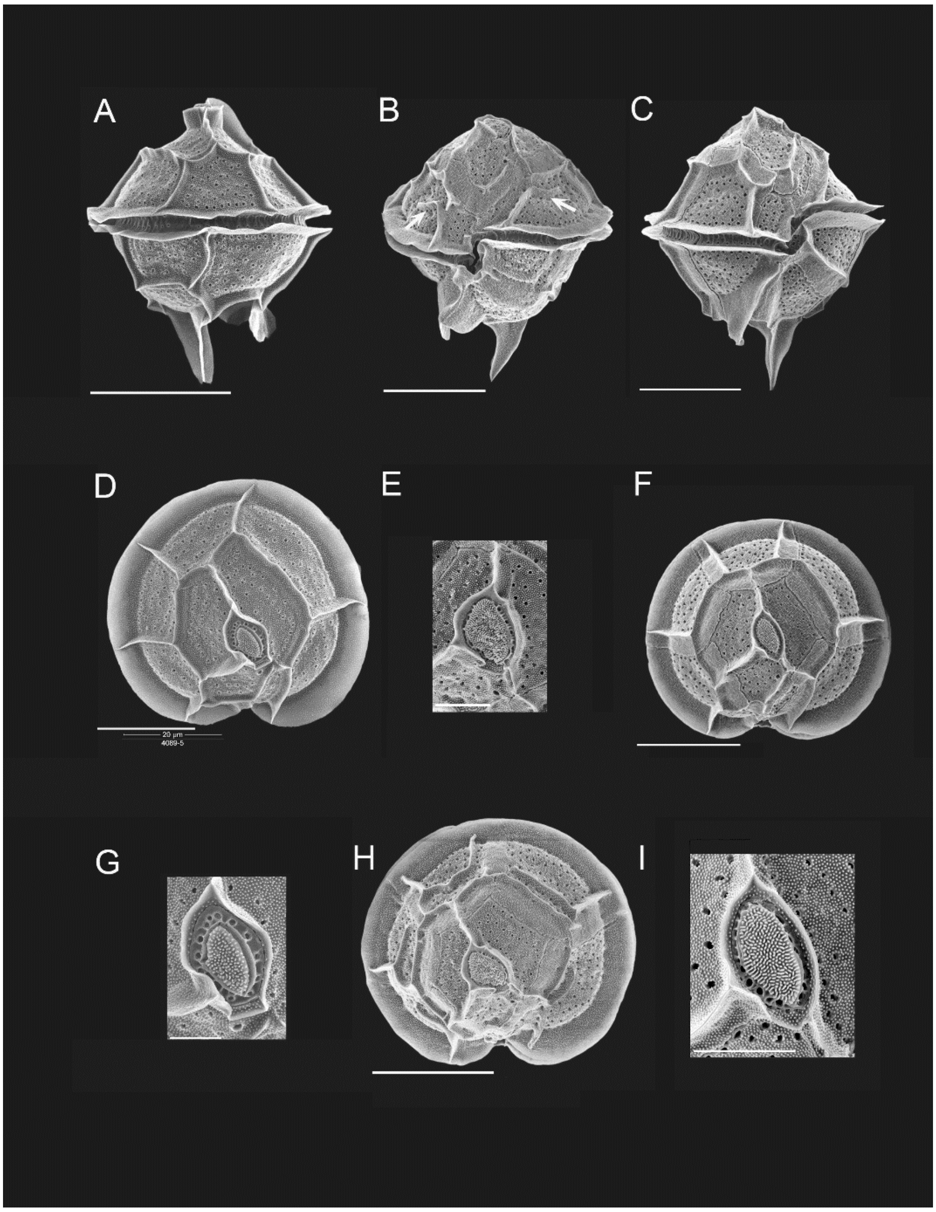

Plate 4. SEM photographs of large cells of *Pyrodinium bahamense* cells from Bioluminescent Bay (Puerto Rico), showing different development of lists and spines while none of them show an attachment pore on the apical pore plate PO. (A). Right lateral view. Note narrow growth bands and a tall apical process formed by extensions of plates 2′, 3′ and 4′. Same cell as in (D) and (G). (B). Ventral view. Arrows show the ridges on plates 1″ and 5″. Same cell as E and H. (C). Ventral view. Note the large growth bands, and the absence of ridges on plates as in B. Same cell as F and I. (D). Apical view. Note the narrow growth bands. Same cell as A and G. (E). Apical pore complex of cell in B and H. Note the large size of the cover or closing plate PI. (F). Apical view. Same cell as C and I. (G). Apical pore complex of cell in A and D. Note

that PO is wider than cells in E and I, which have much larger growth bands. (H). Apical view. Note the wide growth bands. Same cell as B and E. (I). Apical pore complex of cell in C and F. Note that PI is smaller than cell in H, which has wider growth bands. Scale bars: 5 µm: G; 10 µm: E, I; 30 µm: A-D, F, H.

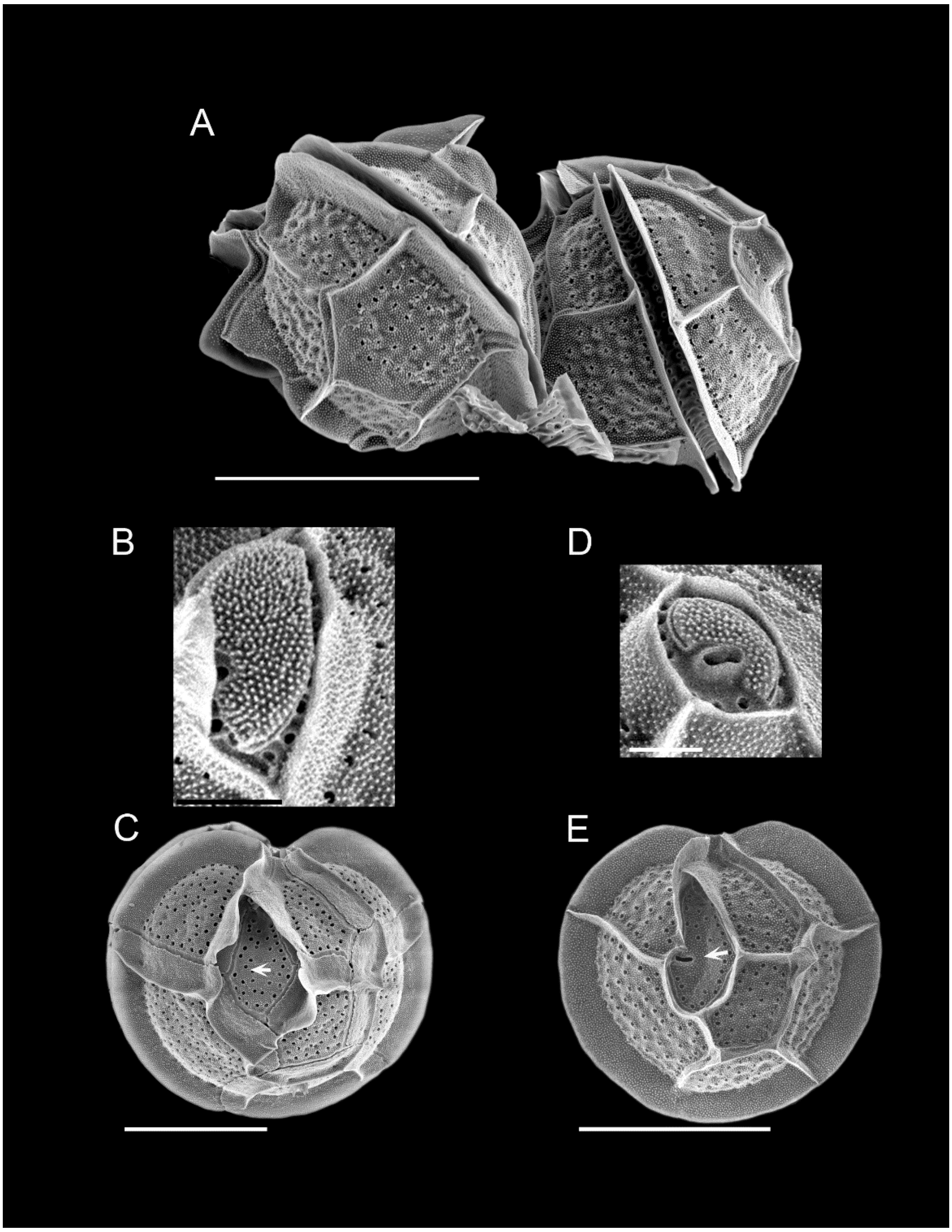

Plate 5. SEM photographs of cells of *Pyrodinium bahamense* showing different development of lists, spines, apical pore complex and attachment pore on the posterior sulcal plate Sp. (A). Two cells from the Philippines (Masinloc Bay). Left cell has larger lists, especially bordering the apical plates. (B). Apical pore complex of the left cell in

A. Note a larger PI, smaller attachment pore, corresponding to a larger list development. (C). Antapical view of a cell from Bioluminescent Bay with no attachment pore on Sp (arrow). Note the smaller and more numerous pores on thecal plates as well as much wider growth bands than those in cell in C. (D). Apical pore complex of the right cell in A. Note a smaller PI, larger attachment pore, corresponding to almost no list development. (E). Antapical view of a cell from the Philippines (San Pedro Bay) with attachment pore on Sp (arrow). Note the larger pores on thecal plates as well as much narrower growth bands than those in cell in C. Scale bars: 5 μm: B, D; 30 μm: C, E, I; 40 μm: A.

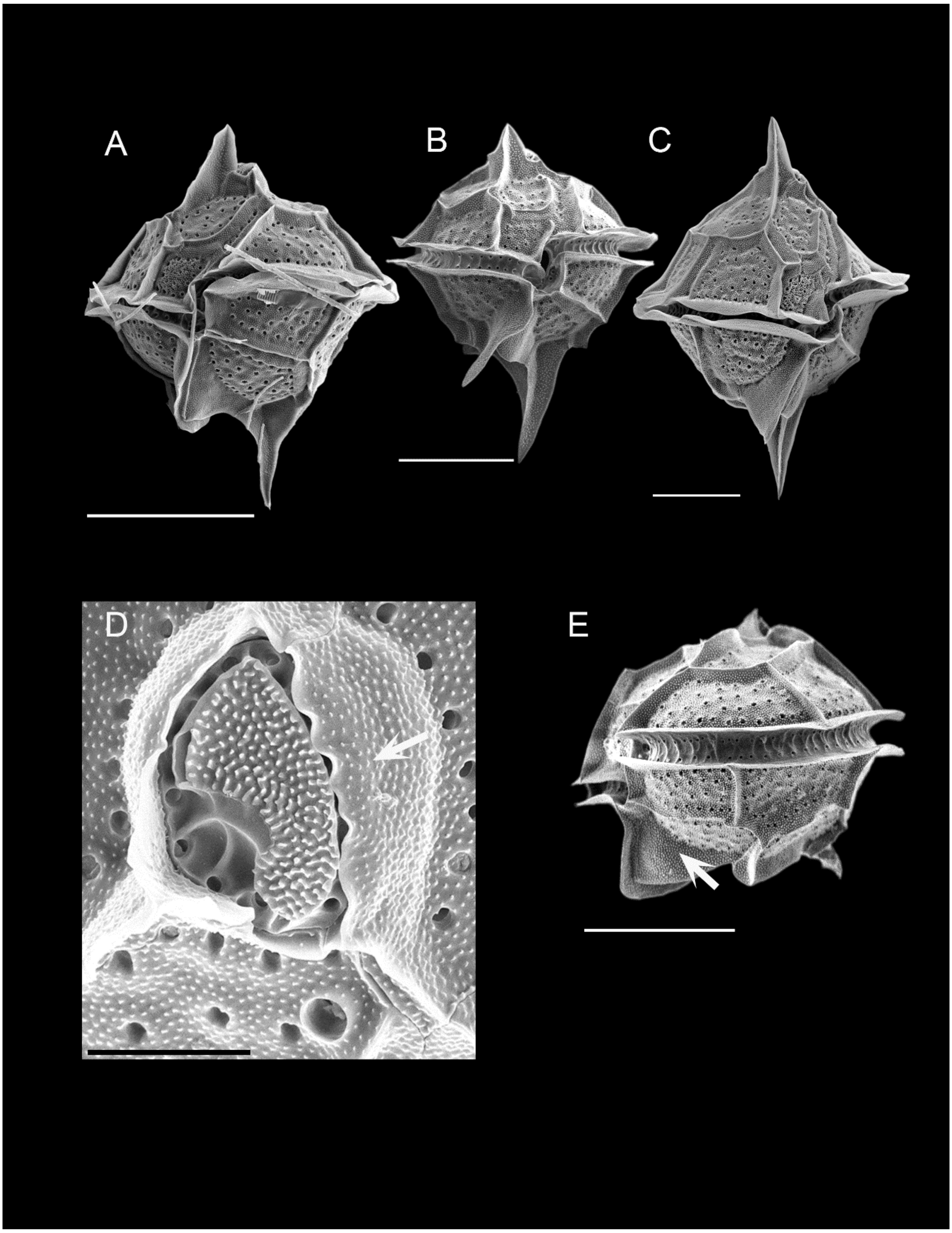

Plate 6. SEM photographs of cells of *Pyrodinium bahamense* cells showing different development of lists, spines and body shape and size. (A). Ventral view of a cell from Ciénaga de los Vásquez (Colombian Caribbean). Note the long apical and antapical spines. Same cell as in D. (B). Ventral view. Small cell from the Philippines (San Pedro Bay). Note the “roundish” cell body and the long lists and spines. (C). Ventral view.

Small cell from the Philippines (Masinloc Bay). Note the long lists and spines. (D). Apical pore complex of cell in A. Note there is no attachment pore. The arrow shows the spinulae on the apical list on plate 2′, similar to the spinulae on all the thecal plates. (E). Left lateral view of a cell from Qatar. Note the large thecal pores and the dissimilar development of lists. Scale bars: 5 μm: D; 20 μm: B,C,E; 30 μm: A.

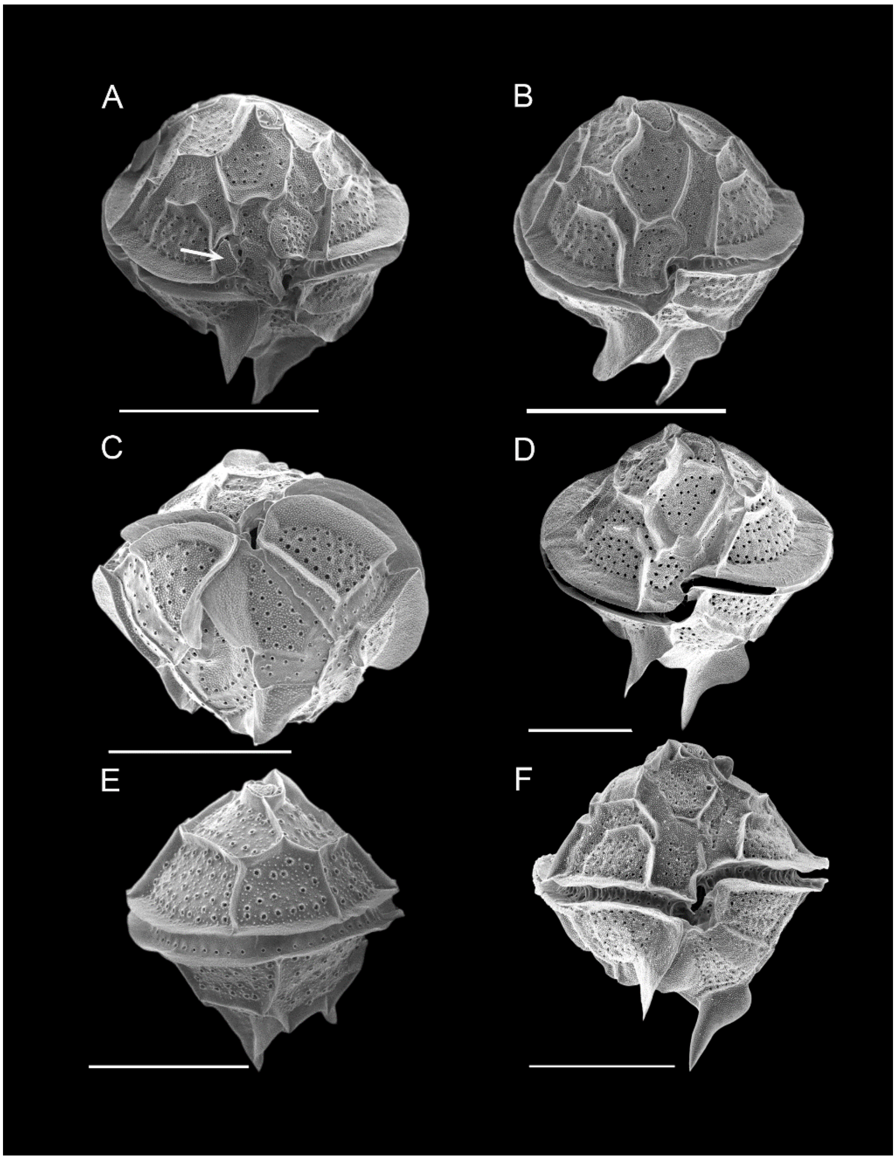

Plate 7. SEM photographs of cells of *Pyrodinium bahamense* cells showing different development of lists, growth bands, and thecal pore size. (A). Ventral view of a cell from the Philippines (San Pedro Bay). Note the differences in pore size development growth bands, and the apparent extra apical pore PI to the left of plate 6″ (arrow). Planozygote? See text. (B). Ventral view of a cell from the Philippines (San Pedro Bay). Note similar growth band development as the cell from Qatar in C. (C). Ventral view of

a cell from the Philippines (San Pedro Bay). Note the unusual pores on the growth bands (D). Ventral view of a cell from Qatar. Note the large growth bands and ridges. (E). Right lateral view of a cell from the Philippines (San Pedro Bay). Note the large thecal pore, the lack of growth bands while there is some list development. (F). Ventral view of a cell from Qatar. Note the large growth bands, no ridges as shown in D. Scale bars: 20 µm: E; 25 µm: D; 30 µm: C, F; 40 µm: A, B.

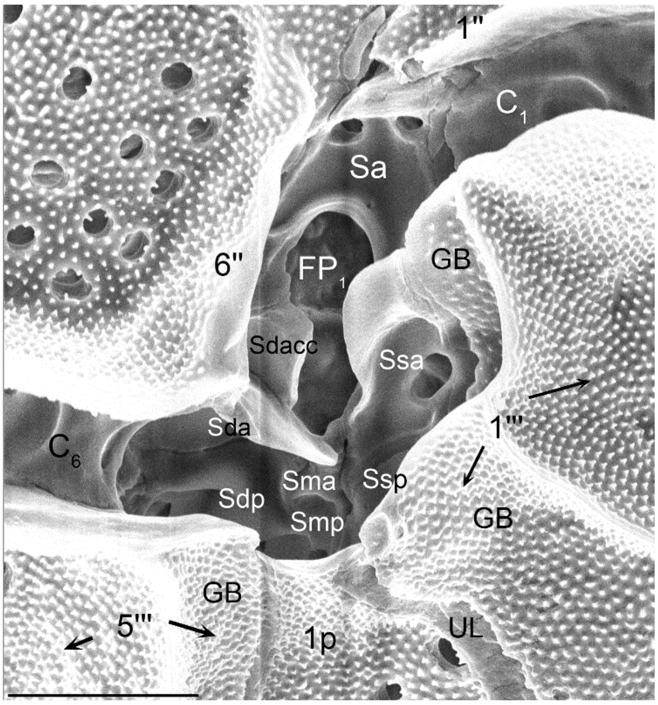

Plate 8. SEM photographs of the ventral area of a cell of *Pyrodinium bahamense* from Bioluminescent Bay (Puerto Rico). Same cell as in Suppl. Plate 1D. GB: growth bands; UL: underlapping; FP: flagellar pore; Sa: anterior sulcal plate; Sdacc: right anterior

accessory sulcal plate (after Balech 1985 notation); Sda: right anterior sulcal plate; Sdp: right posterior sulcal plate; Sma: anterior medial sulcal plate; Smp: posterior medial sulcal plate; Ssa: anterior left sulcal plate (equivalent to 1‴ Kofoidian nomenclature, see text); Ssp: posterior left sulcal plate; C: cingular plates. Scale bar: 5 µm.

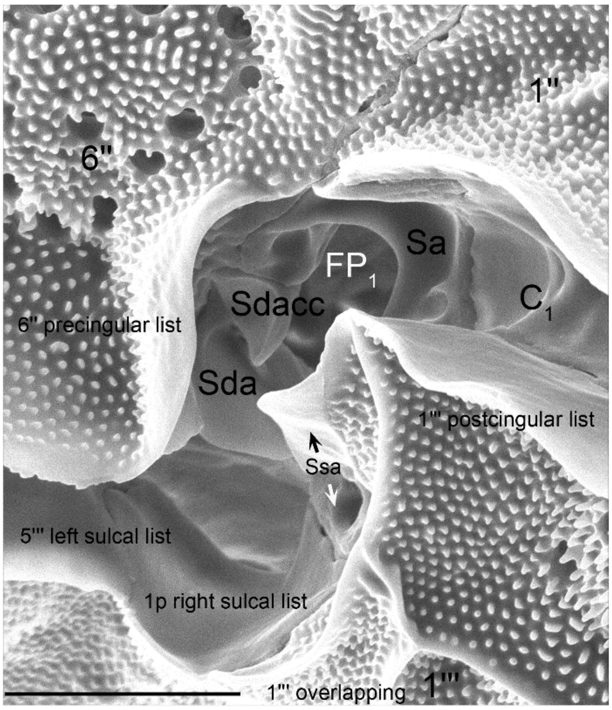

Plate 9. SEM photographs of the ventral area of a cell of *Pyrodinium bahamense* from Bioluminescent Bay (Puerto Rico) as observed from above. Same cell as in Suppl. Plate 1A. GB: growth bands; FP: flagellar pore; Sa: anterior sulcal plate; Sdacc: right anterior accessory sulcal plate (after Balech 1985 notation); Sda: right anterior sulcal plate; Ssa: anterior left sulcal plate (equivalent to 1‴ Kofoidian nomenclature, see text); C: cingular plates. Scale bar: 5 µm.

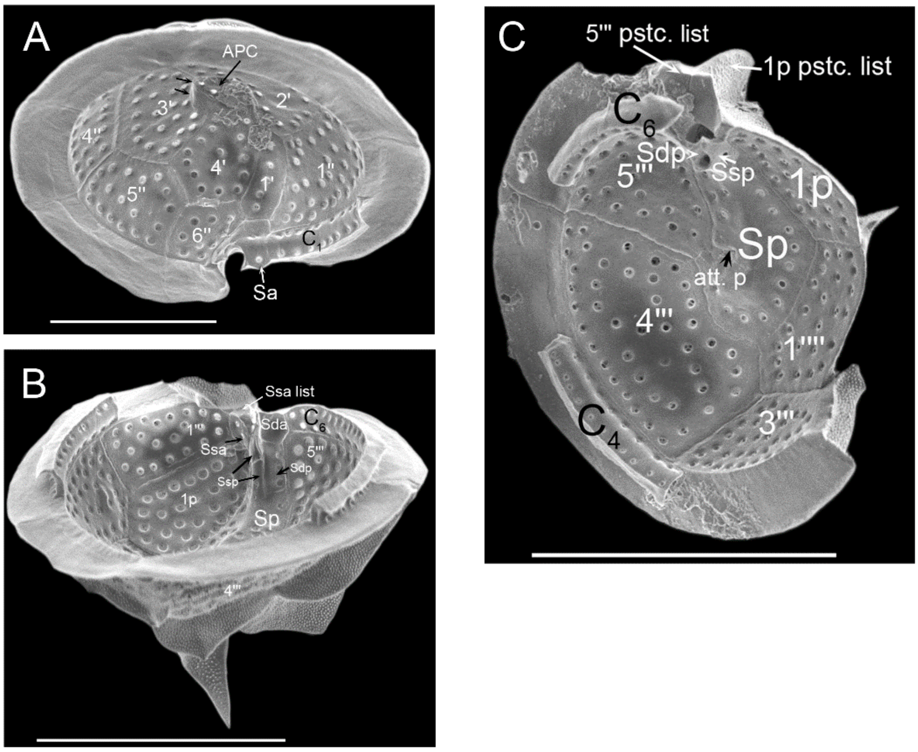

Plate 10. SEM photographs of the inside thecae of *Pyrodinium bahamense* cells from the Philippines (San Pedro Bay). (A). Epitheca, arrows on plate 3′ denote the apical list. (B). Hypotheca, looking inside the ventral area. (C). Part of a hypotheca. The original digital image has been flipped horizontally for easier visualization. Scale bars: 20 μm: A. 30 μm: B, C.

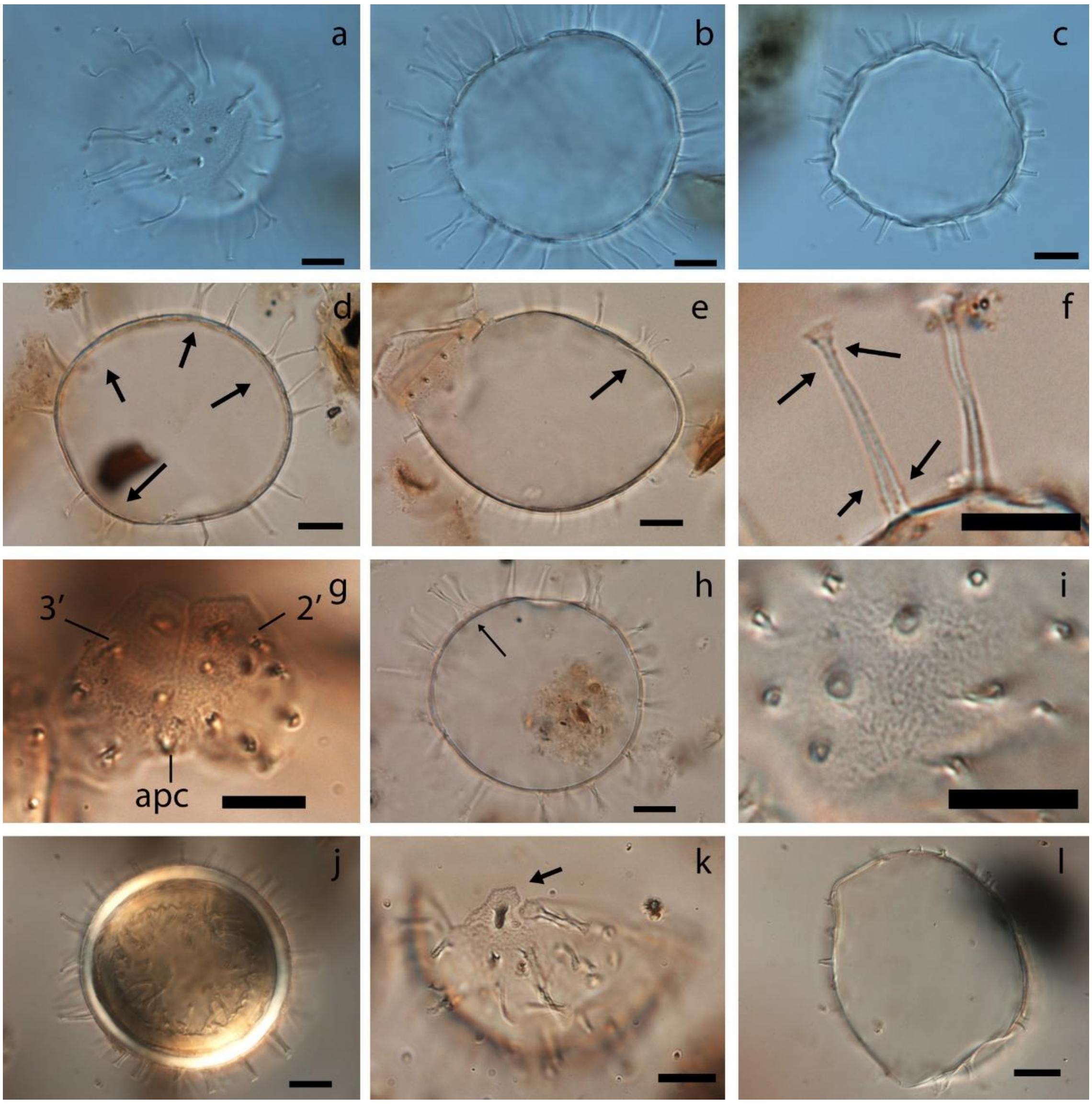

Plate 11. Resting cysts of *Pyrodinium bahamense* (= *Polysphaeridium zoharyi*) collected from different locations. (A-B). Large specimen with long slender processes from the Red Sea (VA200-P). (C). Small specimen with short, tubiform processes from Red Sea (VA200-P). (D). Specimen from Ambon (LC) showing pairs of merged processes (arrows). (E). Specimen from Masinloc Bay (Philippines) showing three processes that were connected by a crest (arrow). (F). Long processes from a cyst of the Bay of Bengal (CIR31G), showing the presence of small spinules on the processes. (G). Group of opercular pieces, corresponding to the apical plates 2′ and 3′ and the apical pore complex (apc), from Safety Harbor (Florida). (H). Specimen from Phosphorescent Bay (PHB4, Puerto Rico), showing two processes connected via a crest halfway along the stalks. (I). Typical texture of cyst wall (Safety Harbor, Florida). (J). Cyst with cell

contents from Safety Harbor (Florida) showing birefringent endospore. (K). Hypocyst from Safety Harbor (Florida) showing anterior sulcal plate, forming the sulcal notch in the epicyst (arrow). (L). Cyst from Safety Harbor (Florida) with reduced processes. Scale bar = 10 μm.

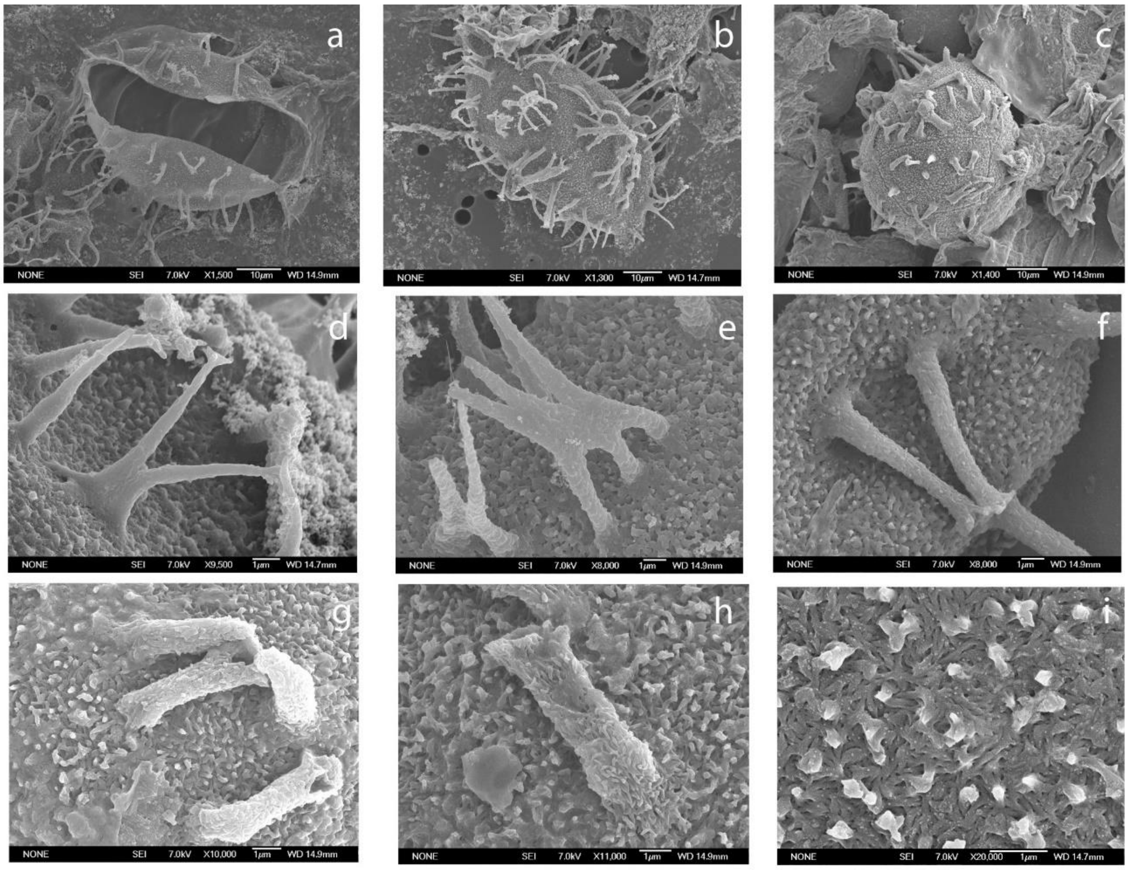

Plate 12. SEM photographs of resting cysts of *Pyrodinium bahamense* (= *Polysphaeridium zoharyi*). (A) Hypocyst (Red Sea, VA200-P). (B) Cyst with long, slender processes (Red Sea, VA200-P). (C) Cyst showing tabulation and intratabular distribution of processes (Safety Harbor, Florida). (D) Processes with aculeate distal ends (Red Sea, VA200-P). (E) Process showing three connected processes (Red Sea, VA200-P). (F-H) Process (Safety Harbor, Florida). (I) Cyst wall texture (Safety Harbor, Florida).

Tables

Table 1 Plankton sampling locations with: number details from Figure 1A; the region; name of the locality; latitude, longitude; sampling date and person who did the sampling; average theca length and width; the number of specimens measured, persons who measured them with LM and persons who did SEM. K.M. = Kazumi Matsuoka, K.N.M. = Kenneth Neil Mertens, J.W. = Jennifer Wolny, T.O. = Takuo Omura, J.R.R. = Juan R. Relox Jr., T.S. = Theodore Smayda, A.R.A. = A.R. Almuftah, E.F.F. = Elsa F. Furio, C.C.M. = Consuelo Carbonell-Moore.

Number on Fig. 1A	Region	Locality	Latitude (°N) (*=approximated)	Longitude (°E) (*=approximated)	Sampling date	Sampled by	Avg theca length (μm)	Avg theca width (μm)	Number of specimens measured	Measured by	SEM by
1	Pacific	Manila Bay, Philippines	14.53*	120.76*	Feb 1992	K.M.	39.78	45.47	12	K.M.	
2	Pacific	Masinloc Bay 1, Philippines	15.51	119.94	21-May-93	J.R.R.	38.56	44.93	207	K.N.M.	
2	Pacific	Masinloc Bay 2, Philippines	15.51	119.94	10-Jul-86	K.M.	46.21	49.24	100	K.N.M.	C.C.M.
3	Pacific	Palawan, Philippines	9.92*	118.77*	NA	E.F.F.	41.67	43.33	12	K.M.	
4	Pacific	Kao Bay, Indonesia	1.10*	127.83*	July 1993	K.M.	37.45	46.03	10	K.M.	
5	Pacific	Palau	7.33*	134.54*	16-Dec-96	K.M.	40.37	48.53	9	K.M.	
6	Indian Ocean	Off Qatar, Persian Gulf	25.29	51.54	30-Sep-08	A.R.A.	55.91	58.28	116	K.M. / K.N.M.	K.N.M.
7	Caribbean	Oyster Bay	18.49*	-77.64*	Dec 2000	T.S.	60.91	60.00	11	K.M.	

		(Jamaica)									
8	Caribbean	Bioluminescent Bay (Vieques Island), Puerto Rico	18.12	-65.37	31-Dec-95	T.O.	57.75	58.87	81	K.M. / K.N.M.	C.C.M.
9	Atlantic	Guatemala (Atlantic coast)	15.71*	-88.62*	30-Jul-90	K.M.	59.60	58.80	10	K.M.	
10	Atlantic	Terra Ceia, FL, USA	27.52	-82.70	14-Jul-03	J.W.	38.55	38.04	34	J.W.	
11	Atlantic	Tampa Bay, FL, USA	27.95	-82.55	22-May-03	J.W.	47.35	43.30	50	J.W.	
12	Atlantic	Indian River Lagoon, FL, USA	28.32	-80.70	16-Aug-02	J.W.	42.10	36.23	50	J.W.	
13	Caribbean	Ciénaga de los Vásquez, Bolívar, Colombia	10.27*	-75.58*	08 Aug-77	C.C.M.	51.57	48.42	7	C.C.M.	C.C.M.
14	Pacific	San Pedro Bay	11.25*	125.02*	29 Nov-03	NA	NA	NA	NA	NA	K.N.M.

Table 2 Sampling locations for cysts of *Pyrodinium bahamense* with: number details from Figure 1B; the region; name of the locality; latitude, longitude; water depth (m); core type; sampling date; reference; average cyst process length; average cyst body diameter and the number of specimens measured.

Number on Fig. 1B	Region	Locality	Latitude N +, S -	Longitude W- E +	Water depth (m)	Core type	Sampling date	Reference	Cyst process length (µm)	Cyst body diameter (µm)	Specimens measured
1	Atlantic	T89-14BC (=sample 6), Angola Basin	-3.51	9.69	868	Boxcore	1989	Dale et al., 2002	11.70	46.60	1
2	Atlantic	Devils Hole (sample 73), Bermuda	32.32	-64.72	22.0	NA	March 1968	Wall and Dale, 1969	11.39	53.73	32
3	Atlantic	Off Castle Harbor Hotel , Bermuda	32.35	-64.69	13	NA	March 1968	Wall and Dale, 1969	NA	50.86	32
4	Atlantic	Castle Harbor, Bermuda	32.37	-64.70	13	NA	March 1968	Wall and Dale, 1969	NA	49.85	32
5	Atlantic	Devils Hole, Bermuda	32.33	-64.72	22	NA	March 1968	Wall and Dale, 1969	NA	51.79	28
6	Atlantic	Smith’s Sound, Bermuda	32.37	-64.66	10	NA	March 1968	Wall and Dale, 1969	NA	54.97	32
7	Caribbean	Phosphorescent Bay (PHB4), Puerto Rico	17.97	-67.02	5	NA	1990	Unpublished	11.13	54.54	22
8	Caribbean	R4596 (GC-6 D), Gulf of Mexico	30.26	-88.97	4.9	Boxcore	17-Sep-91	Edwards and Willard, 2001	9.38	53.13	50
9	Caribbean	R4597 (GC-6 E), Gulf of Mexico	30.24	-88.94	5.5	Boxcore	17-Sep-91	Edwards and Willard, 2001	9.41	54.15	29
10	Caribbean	R4600 (GC-7C), Gulf of Mexico	30.18	-88.96	7.9	Boxcore	17-Sep-91	Edwards and Willard, 2001	9.30	54.83	50
11	Caribbean	MD02-2574, Gulf of Mexico	28.63	-88.22	1963	Calypso core	15-Jul-02	Unpublished	9.21	55.06	9
12	Atlantic	R4974 (Station #9 Buttonwood Sd.), Florida	25.09	-80.47	1.83	Pushcore	10-Nov-94	Wingard et al., 1995	8.53	54.54	1
13	Atlantic	R5256A(4) (SEI 2-97 CB-1 0-2 cm	25.30	-80.34	2	Piston core	5-May-97	Ishman et al., 1996	5.53	51.55	3

		Card Bank), Florida									
14	Atlantic	Site 1 Tampa Bay 11 Sept 2003, Florida	27.91	-82.45	1.0	Boxcore	11-Sep-03	Unpublished	8.13	52.54	50
15	Atlantic	Site 1 Tampa Bay 21 April 2004, Florida	27.91	-82.45	1.0	Boxcore	21-Apr-04	Unpublished	8.36	51.46	18
16	Atlantic	Site 1 Tampa Bay Oct 2004, Florida	27.91	-82.45	1.0	Boxcore	Oct 2004	Unpublished	8.09	51.80	39
17	Atlantic	Site 1 Tampa Bay Feb 2005, Florida	27.91	-82.45	1.0	Boxcore	Feb 2005	Unpublished	7.60	52.74	13
18	Atlantic	Safety harbor, Florida	28.00	-82.67	2.0	Boxcore	14-Aug-09	Unpublished	6.18	50.51	50
19	Atlantic	West Lake 25, Florida	25.20	-80.81	0.7	Hand sampling	17-May-11	Unpublished	7.02	54.20	23
20	Indian Ocean	Persian Gulf 1506 (12)	26.25	55.88	70.0	NA	1961-1969	Bradford and Wall, 1984	8.71	59.14	50
21	Indian Ocean	Persian Gulf 1507 (13)	29.52	49.10	25.0	NA	1961-1969	Bradford and Wall, 1984	9.33	55.19	50
22	Indian Ocean	Persian Gulf 1514 (20)	26.99	51.77	65.0	NA	1961-1969	Bradford and Wall, 1984	9.99	60.47	50
23	Indian Ocean	Persian Gulf 1522 (28)	25.83	55.62	15.0	NA	1961-1969	Bradford and Wall, 1984	9.21	56.58	50
24	Indian Ocean	Persian Gulf 1538 (45)	26.48	56.34	80.0	NA	1961-1969	Bradford and Wall, 1984	9.59	56.16	50
25	Indian Ocean	Musandam Peninsula 1578 (308)	26.12	56.31	10.0	Van Veen Grab	1971-1972	Bradford and Wall, 1984	9.00	51.53	50
26	Indian Ocean	VA01-200P 0-5 cm, Red Sea	16.77	41.32	84.0	Boxcore	1971	Mertens et al., 2009	12.86	49.27	50
27	Indian Ocean	KB6, Kuwait	29.46	47.89	4	TFO corer	2001	Unpublished	9.82	52.88	6
28	Indian Ocean	Circe 22PG 6-9 cm, Bay of Bengal	11.42	83.82	3456	Gravity core	8-May-68	Unpublished	7.94	46.33	21
29	Indian Ocean	Circe 25P 1-2 cm, Bay of Bengal	15.30	83.28	3145	Piston core	11-May-68	Unpublished	10.11	50.08	50
30	Indian Ocean	Circe 27P 1-2.5 cm, Bay of Bengal	15.22	91.23	2651	Piston core	13-May-68	Unpublished	8.29	48.10	41
31	Indian Ocean	Circe 31G 4-5 cm, Bay of Bengal	19.70	92.77	58	Gravity core	15-May-68	Unpublished	12.55	49.60	4

32	Indian Ocean	Circe 39G 4.5-5.5 cm, Bay of Bengal	9.80	83.50	3644	Gravity core	23-May-68	Unpublished	12.07	52.66	23
33	Pacific	Long core 0-2 cm, Ambon	3.65	128.21	26	Pushcore	12-Nov-95	Mizushima et al., 2007	9.45	54.22	50
34	Pacific	St. 10, Ambon	3.65	128.21	26	TFO corer	12-Nov-95	Unpublished	10.00	55.56	38
35	Pacific	Masinloc st.1 2-4cm, Philippines	15.56	119.94	12.3	TFO corer	18-Feb-92	Unpublished	10.51	54.27	50
36	Pacific	Masinloc Bay, Philippines	15.52	119.95	5	TFO corer	18-Feb-92	Unpublished	NA	53.80	33
37	Pacific	Samar Sea, Philippines	11.72	124.97	2	TFO corer	Apr 1989	Unpublished	NA	54.04	9
38	Pacific	St. 55 0-2 cm, Palau	7.21	134.28	3.5	TFO corer	Dec 1996	Unpublished	9.67	53.33	30
39	Pacific	Port Moresby, Papua New Guinea	-9.51	147.20	2	TFO corer	Aug 1992	Unpublished	NA	55.59	34
40	Pacific	Kao Bay (KAB 14A), Indonesia	1.17	127.93	26.3	TFO corer	Dec 1994	Unpublished	9.29	52.54	28
41	Pacific	TEHUA V 3 (DB 15 / 2407-03), Tehuantepec	22.81	-106.45	207.3	Boxcore	Sep 2007	Limoges et al., 2010	10.35	52.80	50
42	Pacific	TEHUA V 14 (DB 23 / 2408-05), Tehuantepec	20.75	-105.61	71.6	Boxcore	Sep 2007	Limoges et al., 2010	11.22	53.13	2
43	Pacific	Acapulco (DB54 / 2427-06), Tehuantepec	16.84	-99.84	24	Boxcore	Sep 2007	Limoges et al., 2010	9.16	58.45	3

Table 3. Coefficient of determination R^2 calculated between environmental parameters and average process length of cysts of *Pyrodinium bahamense*. Significant correlations using the t-test (p<1x10-6) are indicated in bold. SST = sea surface temperature, SSS = sea surface salinity and and σt = seawater density.

	Process length (Total dataset)	Body diameter (Total dataset)	Process length (Atlantic-Caribbean)	Body diameter (Atlantic-Caribbean)	Process length (Pacific-Indian Ocean)	Body diameter (Pacific-Indian Ocean)
Annual SST	+0.03	+0.00	+0.39	+0.01	+0.05	+0.15
Annual SSS	+0.01	+0.06	+0.82	+0.00	+0.00	+0.34
Annual σt	+0.00	+0.05	+0.82	+0.00	+0.00	+0.34
Summer SST	+0.01	+0.10	+0.02	+0.09	+0.01	+0.10
Summer SSS	+0.01	+0.10	**+0.88**	+0.02	+0.00	+0.33
Summer σt	+0.01	+0.06	**+0.88**	+0.01	+0.00	+0.36
Autumn SST	+0.09	+0.01	+0.05	+0.01	+0.06	+0.05
Autumn SSS	+0.01	+0.13	+0.81	+0.01	+0.00	+0.32
Autumn σt	+0.00	+0.09	+0.76	+0.01	+0.00	+0.31
Winter SST	+0.07	+0.01	+0.13	+0.03	+0.02	+0.17
Winter SSS	+0.00	+0.04	+0.67	+0.01	+0.00	+0.37
Winter σt	+0.00	+0.05	+0.70	+0.00	+0.00	+0.31
Spring SST	+0.00	+0.00	+0.53	+0.00	+0.04	+0.33
Spring SSS	+0.01	+0.02	+0.72	+0.00	+0.01	+0.32

Spring σt	+0.00	+0.02	+0.72	+0.00	+0.00	+0.36